# Prognostic Value of Epigenetic Markers for Canine Mast Cell Cancer

by

Shahzar Syed

A Thesis

presented to

The University of Guelph

In partial fulfilment of requirements
for the degree of

Master of Science

in

Biomedical Sciences

Guelph, Ontario, Canada

# ABSTRACT

PROGNOSTIC VALUE OF EPIGENETIC MARKERS FOR CANINE MAST CELL CANCER

Shahzar Syed
University of Guelph, 2021

Advisors:
Dr. Geoffrey Wood
Dr. Brenda Coomber

Canine Mast cell tumors (MCTs) constitute approximately 21% of all canine skin tumors. For intermediate graded MCTs, biological aggressiveness is difficult to predict. Progression in various cancers involves DNA hypermethylation, hypomethylation and epigenetic enzyme dysregulation. Therefore, levels of 5-methylcytosine, 5-hydroxymethylcytosine and associated enzyme expression may predict MCT aggressiveness. A tissue microarray with cores from 244 different tumor samples from 189 dogs was immunolabelled. H-scores were generated using QuPath (v0.1.2) and analyzed with associated patient data. High 5MC, DNMT1, and DNMT3a and low TET2, IDH1, and IDH2 levels were associated with poorer outcome in all canine MCT cases. High 5MC showed the most significance when stratifying cases by dermal and subcutaneous tissue location, and in intermediately graded cases. Therefore, there is potential for these markers to be able to predict more aggressive behavior and identify aggressive cases based on location as well as in intermediately graded MCTs.

**Acknowledgements**

I would like to thank Dr. Brenda Coomber for all of her support and for the knowledge, guidance and patience she has provided in the progress of this thesis. I would also like to thank Dr. Geoffrey Wood for all of his help and guidance as well.

I would like to thank Jodi Morrison who helped train me in histology and IHC.

I would like to thank all the members of the Coomber, Mutsaers, and Viloria-Petit labs past and present who helped in so many ways and who gave so much knowledge and advice during the progress of my work.

I would like to thank my mom, dad, and sister and the rest of my family for their support and constant encouragement.

And finally, I would like to thank my friends who have always been there for me and have always provided me with support and without whom life wouldn't be as fun.

***Declaration of Work Performed***

I declare that this work was conducted by me except for the following:

Lysates of canine cells were provided by Morla Phan (MCT-1 and MCT-2 cells), Nicholas Prevedel (CLBL-1 cells) and Andrew Poon (MDCK cells), all Department of Biomedical Sciences, Ontario Veterinary College, University of Guelph.

The TMA was previously constructed by Britta Knight from the Department of Pathobiology, OVC.

The TMA was sectioned by Susan Lapos from the Histology department of the Animal Health Laboratory, University of Guelph.

The immunolabelled TMA microscope slides were scanned by the Ontario Institute for Cancer Research, MaRS Centre, Toronto, Ontario.

Information on case outcome was collated by Jen Thompson and Britta Knight, Department of Pathobiology, and Karolina Skowronski, Victoria Sabine and Deirdre Stuart, Institute for Comparative Cancer Investigation, University of Guelph.

## Table of Contents

ABSTRACT ..... ii
**Acknowledgements** ..... iii
***Declaration of Work Performed*** ..... iv
**Table of Contents** ..... v
**List of Figures** ..... vii
**List of Tables** ..... ix
**List of Abbreviations** ..... x
**List of Appendices** ..... xii
***LITERATURE REVIEW*** ..... 1
**Mast Cells** ..... 1
**Canine Mast Cell Tumours** ..... 1
*Tumour Stage* ..... 2
*Tumour Grade* ..... 2
*Proliferation Markers* ..... 5
*c-KIT* ..... 7
*Treatment of MCT* ..... 10
**DNA Methylation** ..... 11
*DNA Methyltransferase Enzymes* ..... 11
*TET Enzymes* ..... 14
*Isocitrate Dehydrogenase Enzymes* ..... 17
**Assessing Tumour Biomarkers** ..... 18
*Immunolabelling* ..... 18
*Quantifying Immunolabelling* ..... 21
*Tissue Microarrays* ..... 23
***RATIONALE, HYPOTHESIS AND OBJECTIVES*** ..... 25
***METHODS*** ..... 26
SDS-PAGE and Western Blotting ..... 26
Immunohistochemistry Antibody Immunolabelling ..... 28
Immunolabelling Software Analysis ..... 30
Statistical Analysis ..... 31
***RESULTS*** ..... 33

Primary Antibody Validation ..... 33
TMA Analysis ..... 33
Outcome Analysis for all Cases of Canine MCT ..... 42
Disease-Free Interval and Overall Survival for Dermal and Subcutaneous MCTs ..... 48
Disease-Free Interval and Overall Survival for Canine MCTS by Grade ..... 52
***DISCUSSION*** ..... 56
**Summary and Conclusion** ..... 68
***REFERENCES*** ..... 69
***Appendix*** ..... 75
Appendix 1 - Preparation of Materials ..... 75
Appendix 2 - IHC conditions ..... 77
Appendix 3 - QuPath parameters ..... 78
Appendix 4 – Correlation analysis and t-tests ..... 80

## List of Figures

Figure 1: Western blots showing validation of DNMT1, DNMT3a, and TET2 antibodies used for immunohistochemistry.. ..... 34

Figure 2: Western blots showing validation of IDH1 and IDH2 antibodies used for immunohistochemistry. ..... 35

Figure 3: Brightfield images of TMA cores after IHC showing positive and negative immunolabelling ..... 36

Figure 4: Brightfield images of TMA cores after IHC showing positive and negative immunolabelling. ..... 37

Figure 5: Screen shots from Qu-Path analysis. ..... 39

Figure 6: Brightfield images of TMA cores after IHC showing examples of cores with high and low H-score. ..... 40

Figure 7: Brightfield images of TMA cores after IHC showing examples of cores with high and low H-score. ..... 41

Figure 8: Outputs from X-tile program for determining cut-point for survival analysis. ..... 42

Figure 9: Kaplan-Meier survival curves for all mast cell cancer cases stratified by immunolabelling for 5-methylcytosine (5MC). ..... 43

Figure 10: Kaplan-Meier survival curves for all mast cell cancer cases stratified by immunolabelling for 5-hydroxymethylcytosine (5HMC). ..... 44

Figure 11: Kaplan-Meier survival curves for all mast cell cancer cases stratified by immunolabelling for DNMT1. ..... 45

Figure 12: Kaplan-Meier survival curves for all mast cell cancer cases stratified by immunolabelling for DNMT3a. ..... 45

Figure 13: Kaplan-Meier survival curves for all mast cell cancer cases stratified by immunolabelling for TET2. ..... 46

Figure 14: Kaplan-Meier survival curves for all mast cell cancer cases stratified by immunolabelling for IDH1. ..... 47

Figure 15: Kaplan-Meier survival curves for all mast cell cancer cases stratified by immunolabelling for IDH2. ..... 48

## List of Tables

Table 1: Results of logrank analysis of disease-free interval (DFI) and overall survival (OS) for dermal cases only..... 50

Table 2: Results of logrank analysis of disease-free interval (DFI) and overall survival (OS) for subcutaneous cases only. ..... 51

Table 3: Results of logrank analysis of disease-free interval (DFI) and overall survival (OS) for Patnaik Grade 2 cases only. ..... 53

Table 4: Results of logrank analysis of disease-free interval (DFI) and overall survival (OS) for Kiupel Low Grade cases only..... 55

## List of Abbreviations

| | |
|---|---|
| 5caC | 5-carboxylcytosine |
| 5fC | 5-formylcytosine |
| 5HMC | 5-hydroxymethyl-cytosine |
| 5MC | 5 Methylcytosine |
| AgNORs | Argyrophilic Nucleolus Organizer Regions |
| AML | Acute Myeloid Leukemia |
| BER | Base Excision Repair |
| cAML | Canine Acute Myeloid Leukemia |
| CN-AML | Cytogenetically normal acute myeloid leukemia |
| D-2HG | (R)-2-hydroxygluterate |
| DAB | 3,3'Diaminobenzidine |
| DFI | Disease Free Interval |
| DNMT | DNA Methyltransferase |
| DNMT1 | DNA Methyltransferase 1 |
| DNMT3a | DNA Methyltransferase 3a |
| FcεRI | High Affinity IgE receptor |
| Fe(II) | Iron 2 Oxide |
| FFPE | Formalin Fixed Paraffin Embedded |
| $G_0$ Phase | Quiescent state |
| HGDH | (D)-2-hydroxyglutarate dehydrogenase |
| HNSCC | Head and Neck Squamous cell Carcinoma |
| HR | Hazards Ratio |
| HSC | Hematopoietic Stem Cell |
| IDH1 | Isocitrate dehydrogenase 1 |
| IDH2 | Isocitrate dehydrogenase 2 |
| IgE | Immunoglobulin E |
| IHC | Immunohistochemistry |

| | |
|---|---|
| IL-3 | Interleukin 3 |
| ITD | Internal Tandem Duplications |
| LN | Lymph Node |
| MCT | Mast Cell Tumour |
| MCT1 | Adherent Mast Cell Tumour Cell Line |
| MCT2 | Suspension Mast Cell Tumour Cell Line |
| MDS | Myelodysplastic Syndrome |
| MST | Median Survival Time |
| NOR | Nucleolar Organizer Regions |
| OS | Overall Survival |
| PVDF | Polyvinylidene Difluoride |
| rRNA | ribosomal RNA |
| SCF | Stem Cell Factor |
| TCGA | The Cancer Genome Atlas |
| TDG | Thymine DNA Glycosylase |
| TET | Ten-Eleven translocation |
| TF | Transcription Factor |
| TMA | Tissue Microarray |

## List of Appendices

Appendix 1 - Preparation of Materials ..... 75
Appendix 2 - IHC conditions ..... 77
Appendix 3 - QuPath parameters ..... 78
Appendix 4 - Correlation analysis and t-tests ..... 80

## *LITERATURE REVIEW*

### Mast Cells

The most striking feature of mast cells is their abundant cytoplasmic granules, leading Paul Ehrlich to call them "mastzellen", believing the granules were the product of overfeeding and that they functioned to nourish the surrounding tissue. Since their discovery by Ehrlich in 1878, the functional implications of mast cells have steadily changed. These cells are derived from $CD34^{+}$ progenitor cells found in the bone marrow which then enter circulation to fully develop into differentiated and phenotypical identifiable mast cells in the presence of stem cell factor (SCF) and various cytokines and factors in their destined connective tissue or mucosal tissue sites (Valent et al., 2020). Mast cells are often found in connective tissue underlying epithelium directly in contact with foreign antigens (Da Silva et al., 2014). Mast cells are most commonly known for their immunoglobulin E (IgE) dependant allergic reaction, although IgE independent activation also occurs. Allergens bound to IgE interact and crosslink with the high affinity IgE receptor (FcεRI) on the mast cell leading to a signal cascade that causes the release of various biologically active factors such as heparin, histamines and cytokines from the mast cell and its many cytoplasmic granules. Mast cells are multifunctional cells that not only have action in inflammation and immune response, but can also become neoplastic.

### Canine Mast Cell Tumours

Mast cell tumors (MCTs) are a prevalent neoplasm in dogs, and account for up to 21% of all skin tumors. Dogs that present with MCT are generally between the age of 7.5 and 9 years, with most of the neoplasms occurring in the dermis and subcutaneous tissue (Garrett, 2014; Welle et al., 2008). Although MCTs can arise in any breed, certain breeds appear to have a

higher prevalence such as pugs, golden retrievers, Boston terriers, Labrador retrievers and boxers; the cause of MCT development and its progression is, however, not well understood (Garrett, 2014). There is a wide variability in the biological behavior of canine MCT ranging from benign, which are easily treated and tolerable, to highly aggressive and metastatic, which have very poor outcomes (Kiupel et al., 2011). Although the majority of MCTs which present as lower grade can be successfully treated through surgical intervention alone with low chance of recurrence, aggressive and metastatic MCTs have a poor prognosis but at times it can prove challenging to differentiate them from the less aggressive MCTs (Sledge et al., 2016).

*Tumour Stage*

There is constant debate over the staging of canine mast cell tumours. For instance, whether stage 2 (single confined dermal tumour with regional lymph node involvement) yields better prognosis compared to stage 3 (multiple, large, infiltrating dermal tumours with or without regional lymph node involvement) (Murphy et al., 2006). It seems most effective to conduct lymph node (LN) aspiration for determining regional lymph node metastasis regardless of single or multiple tumours (Garrett, 2014; Murphy et al., 2006; Warland et al., 2015; Welle et al., 2008). However, the usefulness of assessing lymph node (LN) metastasis is still debated, as some studies find that tumour stage is associated with grade and poorer prognosis while other studies report no difference in survival for cases with LN involvement (Krick et al., 2009; Warland et al., 2015; Welle et al., 2008). Hence, tumour grade is still considered the gold standard in determining tumour prognosis (Krick et al., 2009; Sledge et al., 2016).

*Tumour Grade*

The Patnaik grading system divided canine MCTs into grades 1 to 3 based on various histomorphologic characteristics (cellularity and cellular morphology, mitotic index, extent of tissue involvement, and stromal reaction) (Patnaik et al., 1984). Grade 1 MCTs were defined as well differentiated normal mast cells with round nuclei, medium sized granules, no mitotic figures and are confined to the dermis and don't invade the surrounding tissues (Patnaik et al., 1984). Grade 2 MCTs were defined as being moderately to highly cellular, round to ovoid cells with round to indented nuclei with scattered chromatin, distinct cytoplasm and intracytoplasmic granules, cells extended to the lower dermis or subcutaneous tissue and occasionally extending deeper into the tissue, and rare mitotic cells ranging from zero to two per high power field (Patnaik et al., 1984). Grade 3 MCTs were defined as being highly cellular and having pleomorphic mast cells, with indented to round nuclei and one to multiple prominent nucleoli, arranged in sheets that replace the subcutaneous tissue and underlying tissues and having three to six mitotic figures per high power field (Patnaik et al., 1984). Based on this system, the grade 1 tumors are often benign and have good long term prognosis and are normally cured using surgical excision and grade 3 tumours are more likely to metastasize and lead to poor long term prognosis (Sabattini et al., 2015). The ability of the grade 1 and 3 classifications in the Patnaik system to identify MCT with good and poor prognosis respectively was effective, however the nature of the system with parameters that are highly dependent on subjective characteristics led to considerable inter-observer variability and the grade 2 classification often failed to predict the clinical behavior of MCTs, leading to varied prognostication making it uninformative (Kiupel et al., 2011; Sabattini et al., 2015).

Studies have observed more than 60% inter-observer variability in the classification of grade 2 canine MCTs, with around a 50% chance that MCTs classified as grade 2 will lead to MCT related death (Sabattini et al., 2015). The variability of the 3-tiered Patnaik system led to the development of the 2-tiered Kiupel system. This grading system, with more objective parameters for classifying the MCTs as either high grade or low grade, improved the consistency of the observers to 96.8%, and showed good prognostic ability (Sabattini et al., 2015). High grade MCT were defined as having at least one of the following characteristics: a minimum of seven mitotic figures in 10 high power fields, three cells with at least three or more nuclei per cell in 10 high power fields, or at least three highly irregular nuclei with highly atypical indentations and segmentation, anisokaryosis and karyomegaly (Kiupel et al., 2011).

Due to the subjectivity of the criteria to grade MCTs using the Patnaik system many studies find a large majority of the cases being graded as intermediate grade 2, as much as 80% of the total cases where up to 25% of grade 2 cases succumb to MCT related death (Horta et al., 2018). Kiupel grading criteria has a higher degree of reproducibility and a lower degree of interobserver inconsistency due to more objective grading criteria, and helps to divide the often ambiguous MCT cases given a Patnaik grade 2 grade into high or low Kiupel grades (Horta et al., 2018; Stefanello et al., 2015). This also allows a more accurate prognosis of subcutaneous MCTs as increased mitotic figures are statistically more indicative of aggressive subcutaneous MCTs; historically they would be given a Patnaik grade 2 due to their location despite having lower rates of reoccurrence and metastasis compared to similar graded cutaneous MCTs (Thompson, Pearl, et al., 2011). Regardless of grading system employed, studies show up to 40% of canine patients in high grade tumours have prolonged survival and more than 15% of

MCTs designated as low grade die due to MCT, supporting the requirement for other prognostic factors be used alongside grading (Horta et al., 2018; Stefanello et al., 2015). In a retrospective study conducted by Stefanello et al. when they looked at Patnaik grade 2 tumours, 16.5% of the dogs had nodal or distant metastases and prevalence of metastasis did not differ greatly when the Patnaik grade 2 dogs were classified into either high (14.6%) or low (16.9%) Kiupel grades. Thus, regardless of the grade, some MCT progress to aggressive and metastatic lesions (Stefanello et al., 2015). While grading is useful for the extremes such as non-aggressive grade 1 tumours and highly aggressive grade 3 tumours in the Patnaik scheme, as well as the extremes in each low and high grade of the Kiupel system, to further understand and predict the biological aggressiveness of the intermediate graded MCTs additional prognostic markers are used to supplement grade. Such molecular markers as c-kit mutation status and Kit immunostaining patterns, or proliferation markers such as Ki67, argyrophilic nucleolus organizer regions (AgNORs), and mitotic index are frequently employed along with tumour grading (Halsey et al., 2017; Warland et al., 2015).

*Proliferation Markers*

Tumours develop due to a disturbance in the balance of cellular replication and cell death, the resulting increased cellular proliferation leading to the growth of a tumour. Therefore, markers for proliferation can indicate how many and how fast cells are replicating (Kiupel & Camus, 2019). Mitotic index is a commonly used indirect measure of cellular proliferation and has been shown to be a prognostic factor for predicating biological behaviour for cutaneous and subcutaneous canine MCTs, and can predict patient survival independent of tumour grade (Romansik et al., 2007; Thompson, Yager, et al., 2011; Warland et al., 2015).

Mitotic index is the ratio of mitotic figures in the overall cell population and is calculated by counting the number of mitotic events in 10 High Power microscope fields, where the high power is 400x magnification and field area is 2.7mm$^2$ (Romansik et al., 2007; Warland et al., 2015).

Ki-67 is a protein that is expressed only in the nuclei of cells undergoing the stages of the cell cycle and mitosis (Scholzen & Gerdes, 2000). Cells that are unstimulated or are in a quiescent state ($G_0$ phase) are negative for Ki-67 expression and therefore IHC immunolabelling will yield negative results. Cells in the $G_1$, S, $G_2$ and M phases express increasing levels of Ki-67 and it reaches its highest level of expression in metaphase (Scholzen & Gerdes, 2000).
Ki-67's complete function is still being studied however it has multiple activities during cellular replication. Ki-67 is important in the compaction of heterochromatin as well as in the organisation of heterochromatin, and facilitates the organisation and association of several proteins of the perichromosomal layer with the heterochromatin during mitosis (Booth et al., 2014; Sobecki et al., 2016). Ki-67 immunolabelling will determine the number of cells progressing through the cell cycle therefore it will give information on the fraction of cells that are undergoing replication which is referred to as the growth fraction (Scholzen & Gerdes, 2000).

Nucleolar organiser regions (NORs) are nucleolar substructures present in the nucleus of cells where they are involved in the transcription of ribosomal RNA (rRNA). They are termed argyrophilic (AgNOR) for their ability to be visualised when stained with silver based salts due to the numerous disulphide bonds present between the closely associated proteins which have a high affinity for silver ions (Bostock et al., 1989; Webster et al., 2007). Since the AgNORs are

involved in rRNA transcription they ultimately contribute to the regulation of protein synthesis. Cells with a shorter cell cycle would need a greater generation of ribosomes to facilitate rapid protein synthesis, therefore an increase in the presence/number of AgNoRs would be expected. Although AgNOR score is shown to be associated with the cell doubling time (where generation time is inversely correlated with average number of AgNORs per nucleus) it cannot indicate the phase of the cell cycle. There is still baseline presence of AgNORs in non-replicating cells due to homeostatic protein synthesis activity (Webster et al., 2007), therefore AgNOR score cannot differentiate between cycling and noncycling cells (Van Diest et al., 1998). Thus, an AgNOR score is used to indirectly infer the proliferation rate of cells and can give information on how fast a population of cells is replicating, especially when used in tandem with other markers for proliferation (Kiupel & Camus, 2019; Van Diest et al., 1998). However, with any of the above proliferation markers, the index or score obtained depends on the selected area of the tissue section evaluated. As well, there are difficulties with highly granulated MCTs as well as bizarre nuclei that may resemble mitotic figures (Kiupel & Camus, 2019).

*c-KIT*

While the causes of MCT development are not fully understood, out of the multiple contributing factors identified, mutation in the proto-oncogene c-kit is often implicated in more aggressive MCTs (Letard et al., 2008). c-kit is a gene that encodes for the transmembrane tyrosine kinase receptor for stem cell factor KIT (Gil Da Costa, 2015). Mutations in the c-kit gene are reported in up to 15% of all cutaneous MCTs and up to 35% of higher grade canine MCTs (Gil Da Costa, 2015). The most common mutation is the internal tandem duplications (ITDs) in the juxtamembrane domain encoded by exon 11 (Letard et al., 2008), although mutations in

exons 8, 9 and 17 are also reported (Gil Da Costa, 2015). Juxtamembrane domain mutations led to autophosphorylation and constitutive activation of the KIT receptor, independent of ligand binding, resulting in unregulated downstream signal transduction of multiple proliferation and cell survival pathways such as RAS/MAPK, PI3-K and SFK pathways (Da Costa, 2015; Letard et al., 2008). Therefore, the progression and development of some canine MCTs is considered to be associated with mutations in the c-kit gene. Studies show that c-kit exon 11 ITDs are associated with more aggressive MCTs outcome such as metastasis or death (Letard et al., 2008). c-kit ITDs are a good predictor for progression free survival and are significantly correlated with proliferation markers such as Ki67 and AgNOR, and with a higher grade (Horta et al., 2018; Webster et al., 2007; Zemke et al., 2002). Due to this, the mutations in c-kit were proposed as a useful aid in prognostication of more aggressive canine MCTs. A study by Takeuchi et al. found that there was a significant difference between PFS based on c-kit mutation status in univariate analysis, but found no significance for c-kit status as an independent prognostic factor (Takeuchi et al., 2013). Horta et al. found ITDs in exon 11 were associated with grade and markers of proliferation, but the presence of this mutation was only predictive of outcome in univariate analysis (Horta et al., 2018). Although it is an objective marker, mutant c-kit shows low prevalence in subcutaneous canine MCTs; although these are generally benign, a subset is biologically aggressive (Horta et al., 2018; Thamm et al., 2019). However, a study involving 60 subcutaneous canine MCTs that included biologically aggressive cases found no exon 11 ITDs (Horta et al., 2018; Thamm et al., 2019; Thompson, Yager, et al., 2011). KIT receptor immunolabelling pattern has also been evaluated for its ability to

determining MCT outcome (Horta et al., 2018). Therefore, the ability of ITDs in exon 11 to be independent prognostic markers for canine MCT is still uncertain.

There are three immunolabelling patterns for Kit identified. Pattern I is associated with more benign MCTs, and labelling is membrane associated; pattern II is focal to stippled cytoplasmic labelling, and pattern III is diffuse cytoplasmic labelling (Halsey et al., 2017; Horta et al., 2018). Using KIT immunolabelling patterns for prognosis yields variable results. In a study by Kiupel et al. in cutaneous MCTs, Kit staining patterns II and III were significantly associated with shorter overall survival and an increased rate of local recurrence, and 25.6% and 38.5% of dogs with kit staining pattern II and III, respectively, died due to mast cell disease. (Kiupel et al., 2004). In a study by Thompson et al., of 60 subcutaneous cases, KIT staining pattern III was significantly associated with increased odds of local recurrence and metastasis compared to KIT staining pattern I, however, there was no significant difference between patterns III and II, or patterns II and I (Thompson, Yager, et al., 2011). In a study conducted by Horta et al. which included 149 dogs with MCTs (subcutaneous and cutaneous) they found that cases with KIT pattern III had decreased overall survival compared to pattern I, but found no significant difference between pattern III and II, and pattern II and I (Horta et al., 2018). A study conducted by Giantin et al. included 60 Cutaneous MCT cases. They found that KIT staining pattern III was significantly associated with Kiupel High grade and patterns III and II were associated with Kiupel High grade and Patnaik grade 2 and 3 (Giantin et al., 2012). However, KIT staining patterns III and II were not good predictors of worse prognosis but KIT pattern I was associated with good prognosis (Giantin et al., 2012). In a study conducted by Costa Casagrande et al. which included 81 MCT cases, they did not find any significant differences between the KIT

staining patterns associated with Patnaik grading or recurrence and they did not see any significance in KIT staining pattern as predictor for aggressive disease outcome (Costa Casagrande et al., 2015). However, they found pattern I was significantly indicative of a good prognosis therefore there is value to using membrane Kit localization to rule out aggressive tumours (Giantin et al., 2012;Horta et al., 2018; Kiupel et al., 2004; Thompson, Yager, et al., 2011).

*Treatment of MCT*

Surgical resection is the standard of care for treatment of MCTs, where the local tumour is excised with surgical margins of 3 cm laterally and one fascial plane deep, although studies identify that such wide margins are not always necessary for lower graded tumours (Selmic & Ruple, 2020). Fulcher et al. found that of 23 MCTs (4 grade 1, 19 grade 2) only 2 grade II MCTs were not fully excised with 2cm lateral margins and one fascial plane deep (Fulcher et al., 2006). There was no local recurrence of MCT in any of the dogs during the follow-up interval however 3 dogs from the complete excision grade 2 group had de novo MCT development which Fulcher et al. noted was a rate comparable to studies conducted with wider surgical margins (Fulcher et al., 2006). Itoh et al. saw that of 25 small MCTs with Kiupel low grade undergoing proportional margin resection (surgical margin proportional to tumour diameter ranging from 0.3cm - 2.6cm) 20 had complete margins and no local recurrence at the initial surgery site (Itoh et al., 2021). Depending on the grade, the proliferation markers, and whether wide surgical excision is possible versus incomplete margins, this will guide what treatments and combinations of treatments will be administered (Garrett, 2014). In the case of incomplete surgical margins or where wide surgical margins are not possible in lower graded tumours, the

residual disease is treated with radiation therapy (Warland et al., 2015). In the case of nonresectable tumours with high grade or high risk of metastasizing, treatments with chemotherapeutics such as vinblastine, prednisolone, and lomustine are used. Adjunctive therapy using tyrosine kinase inhibitors (TKIs) such as toceranib and masitinib, is used in the treatment of high grade tumours and lower graded tumours with high risk of progression (Warland et al., 2015). Thamm et al. studied high risk intermediate grade and high grade MCTs and observed that implementation of a combination of vinblastine and prednisolone after complete or incomplete surgical excision showed better overall survival and disease free progression with tolerable adverse reactions compared to surgery alone (Thamm et al., 2006).

Single agent treatment with Palladia (toceranib) a TKI which inhibits KIT, platelet derived growth factor receptor β, and vascular endothelial growth factor receptor 2 was administered to dogs with Patnaik grade 2 and 3 MCTs compared to placebo group in a study conducted by London et al. (London et al., 2009). Palladia treated dogs had a 6.5 times higher objective response and significantly longer time to progression compared to placebo treated dogs; dogs with c-Kit positive tumours were more likely to respond in the Palladia treatment group (London et al., 2009). Therefore, proper biomarker identification is important in identifying effective course of treatments. Depending on the possibility of complete surgical excision, grade, level of markers such as; Ki-67, AgNORs, MI, and KIT staining patterns and c-KIT mutational status will guide various combined and single treatment options (Olsen et al., 2018).

**DNA Methylation**

*DNA Methyltransferase Enzymes*

Epigenetics allows for an adjustment in gene function and activity without the alteration of DNA sequence (Meng et al., 2015). In vertebrates the most common epigenetic modification is DNA methylation; DNA methylation modifications occur by covalently adding a methyl group by DNA methyltransferase (DNMT) enzymes onto the 5' carbon of the cytosine base on its pyrimidine ring. This occurs most commonly at CpG dinucleotides which can be found occasionally in groups referred to as CpG islands (Meng et al., 2015). The mammalian DNMT family of enzymes consists of 3 enzymes. DNMT3a and DNMT3b are responsible for establishing methylation patterns on the DNA and are therefore termed de novo DNMTs (Tajima et al., 2016). DNMT1 is responsible for maintaining the DNA methylation patterns and status after DNA replication and repair therefore it is referred to as a maintenance type DNMT (Tajima et al., 2016).

DNMT3s are very active in the early embryonic development of mammals and have important roles in establishing methylation patterns involved in X-chromosome inactivation, and regulation of gene expression (Chen et al., 2003; Tajima et al., 2016). Methylation leading to the inhibition of transcription has long been studied. Gene silencing can occur by methylation of the CpG islands associated with the promoter regions of genes leading to the prevention of the binding of transcription factors (Greenberg & Bourc'His, 2019). DNA methylation is often dysregulated in cancers, especially in hematopoietic malignancies of the myeloid cell lines such as acute myeloid leukemia (AML) and myelodysplastic syndrome (MDS) (Dexheimer et al., 2017). Mast cells are fairly heterogenous. They differentiate and mature once they have migrated to their respective tissue sites, and cells from each location have differential expression of factors that are released. Thus mast cells upregulate or downregulate

different genes depending on which location they settle in, and therefore need mechanisms to activate and supress relevant genes depending on the situation (Reszka et al., 2021).

Studies have found that DNMT3a is important in haematopoietic stem cell (HSC) differentiation and self-renewal (Challen et al., 2012). In HSCs lacking DNMT3a there are genes that showed both hypomethylation and hypermethylation and many of the hypomethylated genes were those commonly associated with human hematopoietic malignancies such as Stat1 and Myc (Challen et al., 2012). Of the upregulated genes identified by Challen et al. many were crucial to HSC function and survival, while factors crucial for HSC differentiation were downregulated, therefore pushing HSC towards replication and self-renewal (Challen et al., 2012). When looking at the effects on hematopoiesis of DNMT1 deficient mouse models there was a tendency for HSCs to have difficulty in generating mature myeloid cells, specifically when compared to lymphoid lineages (Trowbridge et al., 2009). Trowbridge et al. found that there was an increase in common myeloid progenitors, granulocyte-macrophage progenitors, and megakaryocyte-erythrocyte progenitors in the S phase of the cell cycle in DNMT1 deficient cells but an overall decrease in myeloid progenitors, suggesting DNMT1 may be important in the differentiation of mature myeloid cells (Trowbridge et al., 2009). Methylation patterns are dysregulated in canine Acute Myeloid leukemias (cAML) as well, presenting as hypermethylation or hypomethylation in different cases compared to healthy control canine cells (Bronzini et al., 2017). That study also found a mutation in a DNMT3 family supporter gene called DNMT3L in the cAML cases (Bronzini et al., 2017). When administering demethylating agents 6-thioguanine and Zebularine, which inhibit DNMT1, Fleshner et. al. found a decrease in DNMT1 levels and hypermethylation as well as apoptosis of canine large T cell leukemia line

CLGL-90 (Flesner et al., 2014). Collectively, these studies indicate aberrant DNMT expression can be found in canine hematopoietic cancers.

Mastocytosis in humans is characterised as a heterogenous disease with the accumulation of dysregulated mast cells and often has expression of mutated KIT similar to in canine MCT (Traina et al., 2012). In a study conducted by Traina et al., 26 cases of human mastocytosis ranging from the less aggressive indolent forms to the more aggressive systemic mastocytosis also showed mutations in genes related to epigenetic mechanisms (Traina et al., 2012). Mutations were found in TET2 which is responsible for hydroxymethylation of DNA (see below) in 23% (6/26) of patients, 13% (3/26) patients had mutations in DNMT3a and 13% had mutations in ASXL1, a transcriptional regulator (Traina et al., 2012). When looking at patients with wildtype expression of TET2, DNMT3a and/or ASXL1 compared to the patients with expression of mutated TET2, DNMT3a and/or ASXL1, the latter had a shorter OS (Traina et al., 2012). DNMT3a control of mature mast cells was also shown in a study by Leoni et al. which found that mature mast cells without DNMT3a expression had an increased ability to proliferate as well as an upregulated production of cytokines and increased degranulation ability in response to IgE (Leoni et al., 2017). This suggests that DNMTs have an important relationship with mast cells as well as the potential of dysregulation in DNMTs leading to increased disease progression in mast cell malignancies, therefore DNMTs could be markers for more aggressive MCTs (Leoni et al., 2017; Traina et al., 2012).

*TET Enzymes*

While cytosine demethylation was initially thought to occur due to the lack of DNMT1 maintenance of methylation after replication, there is also a family of enzymes that facilitate

the active demethylation of DNA (Leonie I. Kroeze et al., 2015; Yin & Xu, 2016). Active DNA demethylation is initiated by the oxidation of DNA 5-methyl-cytosine (5mC) into 5-hydroxymethylcytosine by the Ten-Eleven Translocation (TET) protein family (Leonie I. Kroeze et al., 2015; Yin & Xu, 2016). TET enzymes are also important in development, as during gametogenesis and early embryo development there are large waves of demethylation that allow for the establishment of methylation patterns by the DNMTs for processes such as X-chromosome inactivation (Tajima et al., 2016; Yin & Xu, 2016). The TET family consists of three enzymes: TET1,TET2 and TET3; they catalyze the oxidation of 5mC to 5-hydroxymethyl-cytosine (5hmC) and then further to 5-formylcytosine (5fC) and 5-carboxylcytosine (5caC) in a Fe(II) and α-Ketoglutarate dependant manner (Yin & Xu, 2016). TET enzyme activity leads to demethylation of cytosine either through passive or active demethylation (Ko et al., 2015). In passive demethylation, during DNA replication the daughter strand is copied using the mother strand that contains the oxidized 5hmc, 5fc or 5caC residues. Due to oxidized 5mC residues on the parent strand of the hemi-methylated DNA, DNMT1 is unable to methylate and maintain the methylation mark on the daughter strand, therefore the daughter strand remains unmethylated, which in subsequent DNA replications leads to fully unmethylated DNA at these sites (Ko et al., 2015). In active demethylation, the DNA repair enzyme thymine DNA glycosylase (TDG) recognises 5fC or 5caC as damaged bases that need to be excised, resulting in an abasic site. This then triggers the base excision repair (BER) pathway to repair the sites, inserting unmethylated cytosines in the process, thereby actively removing the methylation from this region of DNA (Ko et al., 2015).

While mutations and dysregulation can occur in any of the three members of the TET family, TET2 is frequently dysregulated and mutated, especially in haematological malignancies and malignancies of myeloid cells (Huang & Rao, 2014; Rasmussen et al., 2015). A study conducted by Montagner et al. used bone marrow progenitors from TET2 deleted mice ($TET^{-/-}$) and wild type mice ($TET^{+/+}$) (Montagner et al., 2016). Mast cell progenitor cells from $TET^{-/-}$ animals showed delayed differentiation into mature mast cells as well as significantly reduced numbers of total mast cells and fully differentiated mast cells after three weeks in vitro. In contrast, $TET^{+/+}$ cultures had >90% mast cell differentiation compared to ~50% for $TET^{-/-}$ in the presence of IL-3. (Montagner et al., 2016). In TET deficient bone marrow cells there was an upregulation of genes that controlled proliferation and cell cycle, and a downregulation in genes that regulate mast cell differentiation and cytokine production (Montagner et al., 2016). Upregulating the activity of the other members of the TET family was able to restore the dysregulation in mast cell differentiation but not in proliferation, which appears to be TET2 dependant (Montagner et al., 2016). The researchers found that the $TET^{-/-}$ cells had an overexpression of transcription factors (TF) which are involved in myeloid differentiation towards granulocytes and mast cells which could explain the dysregulation in differentiation (Montagner et al., 2016). A study be De Vita et al. was conducted to see if loss of TET2 function alongside KIT activation would lead to a more aggressive mastocytosis disease in humans. In an in vitro model they found that silencing of TET2 combined with a KIT D816V mutation led to an increase in the cellular growth and proliferation in the human mast cell leukemia cell line (HMC-1.2) (De Vita et al., 2014). In vivo studies conducted in mice with a KIT D814V mutation, a homologue to human KIT D816V mutation, showed that loss of TET2 and KIT activating

mutation together led to greater organ infiltration and more histologically aggressive mast cell neoplasia compared to just KIT mutation alone (De Vita et al., 2014). However, TET2 deletion alone wasn't sufficient to cause disease in this mouse model (De Vita et al., 2014). Along with increased proliferation, loss of TET2 led to impaired differentiation of mature mast cells from bone marrow mast cell progenitors derived from these mice (De Vita et al., 2014). These data highlight the significance of TET2 in regulating mast cell differentiation and proliferation, suggesting that canine mast cell tumours with reduced expression of TET enzymes could progress to more aggressive disease, be more poorly differentiated and more proliferative.

*Isocitrate Dehydrogenase Enzymes*

Isocitrate dehydrogenase 1 and 2 (IDH1 & IDH2) are metabolic enzymes that have function in the tricarboxylic acid cycle to catalyze the oxidative decarboxylation of isocitrate to $\alpha$-ketoglutarate in the cytosol and the mitochondria, respectively (Huang & Rao, 2014). In humans, mutations in IDHs are most commonly missense mutations occurring at distinct arginine codons, leading to a single amino acid substitution most commonly to histidine (Waitkus et al., 2018). IDH mutations can be seen frequently in gliomas and in as many as 30% of myeloid malignancies including AML (Acute Myeloid Leukemia) (Figueroa et al., 2010). When IDH1 and IDH2 enzymes are mutated it often leads to a gain of function mutation where the enzymes further convert α-Ketoglutarate to (R)-2-hydroxyglutarate (R-2HG or D-2-HG) (Huang & Rao, 2014; Xu et al., 2011). α-Ketoglutarate along with Fe(II) is one of the important cofactors in the function of TET enzymes which allows the oxidation of 5mC to 5hmC. Mutated IDH1 and IDH2 enzymes favor the production of D-2-HG, therefore levels of α-Ketoglutarate are significantly reduced, which will limit the oxidation activity of the TET enzymes (Huang & Rao,

2014; Xu et al., 2011). D-2-HG is an analog to α-Ketoglutarate where a hydroxyl group is substituted in the place of a keto group (Figueroa et al., 2010; Xu et al., 2011). Increasing levels of D-2-HG may also act as an antagonist for the TET enzymes, inhibiting their ability to generate the hydroxymethylation of 5-mC (Figueroa et al., 2010; Xu et al., 2011). In mouse myeloid progenitor cells in vitro, mutant IDH1 and IDH2 expression in the presence of wild type TET2 and elevation of D-2-HG levels produced a significant increase of global 5-mC levels (Figueroa et al., 2010). Figueroa *et al.* also found that many of the hypermethylated DNA regions in these cells were binding motifs for GATA1, GATA2 and EVI1, which are transcription factors that play important roles for the normal differentiation of myeloid cells (Figueroa et al., 2010). When further looking at 32D myeloid cell lines and primary mouse bone marrow cells there was an increase in c-kit expression of approximately 40% in cells with mutant IDH expression compared to wild type cells. As well, a reduced expression of mature myeloid markers Gr-1 and Mac-1 led to an increase in immature myeloid progenitors and impairment of normal myeloid and hematopoietic differentiation, similar to what is observed in TET knockdown mice (Figueroa et al., 2010).

**Assessing Tumour Biomarkers**

*Immunolabelling*

Immunohistochemistry (IHC) in general is used to immunolabel an antigen of interest in cells and tissues with the utilization of an antibody specific to that antigen (Magaki et al., 2019). IHC is most commonly conducted on formalin fixed paraffin embedded (FFPE) tissue (Magaki et al., 2019). The tissue sample is fixed with a formalin solution which prevents the degradation of

the tissue elements and preserves the morphology of the cells (Kim et al., 2016). Embedding the tissue into paraffin wax gives support when sectioning as well as protecting the tissue and allowing it to be safely stored (Kim et al., 2016). Sections are cut from the FFPE tissues at thicknesses of 3-5 micrometers to allow visualization via light microscopy, and are then mounted on microscope slides (Ramos-Vara, 2017).

Once the slides are deparaffinized and rehydrated the first step in the IHC process is antigen retrieval (Magaki et al., 2019). The antigen retrieval step is important due to the fixation process which leads to the cross linking of the amino groups in adjacent molecules disrupting normal protein morphology which can cause the target antigen to be blocked in the tissue and lead to the inability of antibody binding (Kim et al., 2016; Ramos-Vara, 2017). Antigen retrieval can be done with various physical and chemical methods such as through ultrasound or enzymatic digestion of the cross linking, but the most common method is through heat-mediated antigen retrieval (Magaki et al., 2019). Various methods can be used to apply heat such as microwaves, heating plates, water baths, pressure cookers, and autoclaves, but they all generally have the tissue slides immersed in an antigen retrieval solution (Dey, 2018; Kim et al., 2016). Depending on the heating method the time of heating can vary and temperatures can range from 90-120 degrees Celsius; antigen retrieval solution pH can range from 6-10 (Dey, 2018; Kim et al., 2016). However, a lower temperature with a longer time period allows for the breaking of crosslinks while helping to best preserve tissue morphology (Dey, 2018).

After antigen retrieval, a protein blocking step is applied to reduce unwanted background staining due to nonspecific binding of the antibodies. This can be done by using

normal serum from the same species of the secondary antibody, or other agents such as bovine serum albumin or skim milk powder (Kim et al., 2016). An endogenous peroxidase enzyme 'blocking' step is useful when using certain detection systems, and is widely conducted with 3% hydrogen peroxide, which acts to deplete peroxidase enzyme activity in the section (Kim et al., 2016). After blocking, the validated primary antibodies as well as the secondary antibodies and the colourimetric detection system are applied to the slides to allow visualization of the target through light microscopy (Magaki et al., 2019). Primary antibodies can be monoclonal, which bind to a single epitope for a single antigen, or polyclonal, which bind to multiple epitopes of a single antigen and depending on whether a higher specificity or sensitivity is needed will determine the choice of primary antibody (Dey, 2018). Then a secondary antibody which is targeted against the species of the primary antibody is labelled with the detection method of choice (Magaki et al., 2019). A very common label is horseradish peroxidase enzyme which in the presence of diaminobenzidine (DAB) chromogenic substrate allows for visualization as brown reaction product staining (Magaki et al., 2019). Then a counterstain is applied such as hematoxylin to allow for better visualization by contrasting against the chromogens as well as highlighting tissue structure for better tissue identification (Kim et al., 2016).

It is important in the IHC process to implement various controls to ensure accurate target labelling. The best controls to include every time IHC is performed are a negative and a positive control (Magaki et al., 2019). Positive controls are where the tissue is known to contain an antigen that will stain with the antibody and it would be beneficial if is included on the same slide as the tissue of interest so that it can receive the identical IHC conditions (Magaki et al., 2019). The negative control's purpose is to confirm the protocol is not being affected by

nonspecific binding, which is done by applying the exact same protocol to the negative control slide with the same tissue without the use of the primary antibody (Magaki et al., 2019). Along with these controls a non IHC validation will help determine if the antibodies are specific, for example using western blot to validate the antibody can detect the correct antigen for the correct protein which can be validated by the correct molecular weight (Janardhan et al., 2018; Kim et al., 2016).

IHC is a simple technique that does not require advanced equipment to be performed, and it is a valuable method as it can be used to assess the molecular target and its cellular, subcellular, and intercellular compartments as the technique is performed without destroying the histologic architecture (Kim et al., 2016). IHC can be used in pathological diagnosis such by using markers for classification of tumours, and is useful in prognosis for example by analyzing markers for cellular proliferation (Dey, 2018). Because of the many steps involved in IHC there are several factors to consider to make sure optimal staining and antigen detection occur, as any step from tissue fixation to the application of the detection chromagen can lead to problems such as excessive background due to non-specific binding or difficulties in labelling the target antigen (Kim et al., 2016).

*Quantifying Immunolabelling*

Once slides are immunolabelled with the desired antibody the immunolabelling can then be quantified, and the results interpreted. Analysis and scoring of immunolabelled tissue can range from very qualitative approaches where IHC is used just to detect staining, to more quantitative scoring where results can be statistically analyzed (Fedchenko & Reifenrath, 2014). Evaluations of IHC can range from determining the number of positively stained cells, to further

analyzing the ratio of positively stained cells versus the total amount of cells, to then determining the intensity of positively stained cells *e.g.* as weak, moderate, or strong (Fedchenko & Reifenrath, 2014). Beyond this, more complex scoring where there are multiparameter scoring systems such as the Allred-score, immunoreactive score, and H-score may be employed (Fedchenko & Reifenrath, 2014). All of these approaches apply multiple parameters such as percentage of stained cells and levels of staining intensity and generate scores that can be interpreted in statistical analysis (Fedchenko & Reifenrath, 2014).

For example, H-score is given by multiplying the percentage of cells by the value of staining intensity assigned to them from no staining (0), low staining (1), moderate staining (2), and high staining (3) to generate a score from 0 to 300 (Fedchenko & Reifenrath, 2014). Quantifying immunolabelling can be conducted manually, usually by a trained individual or a pathologist, to accurately measure the staining and ensure proper scoring of the tissue as the skill and experience of the observer can influence scoring (Fuhrich et al., 2013). However, the use of digital analysis of slides using software like ImageJ or QuPath includes an aid to allow for easier quantification of immunolabelled tissue (Bankhead et al., 2017; Fuhrich et al., 2013). The analysis software can deconvolute the chromogen staining from the counterstain and background by analyzing the colour of individual pixels from the scanned slide (Bankhead et al., 2017; Fuhrich et al., 2013). Once 'trained' to detect the proper staining, and once staining levels are set, analysis of the tissue can be automated to detect targeted cells and score them all with reproducibility (Bankhead et al., 2017). A comparison was conducted between the scoring ability of a trained pathologist compared to an inexperienced researcher utilizing the ImageJ software for evaluating endometrial biopsies immunolabelled for β3 integrin (Fuhrich et al.,

2013). The case set involved 50 positive and 50 negative examples, and when aided with ImageJ the naïve researcher only scored three of the 100 slides differently from the experienced observer. In comparison, when the same naïve observer used manual scoring, they were unable to correctly score these specimens 50% of the time (Fuhrich et al., 2013). Thus, machine-aided immunolabelling quantification allows for more accurate, rapid, and reproducible assessment of histological slides even with an inexperienced researcher (Bankhead et al., 2017; Fuhrich et al., 2013).

*Tissue Microarrays*

A tissue microarray (TMA) for cancer related research allows for the analysis of hundreds of biological samples in parallel on a single microscope slide (Jawhar, 2009). Several cores from FFPE tissue samples ("donor" blocks) are taken and arranged into holes made in a blank "recipient" paraffin block and tumours from multiple different patients can be included in one block. This allows for high throughput analysis of various molecular markers, generally by IHC (Hassan et al., 2007). In cancer TMA construction, tissue samples need to be collected and then the most representative area of the cancer needs to be determined, generally by a board-certified pathologist. Then core biopsies of diameters ranging from 0.6 mm up to 2.0 mm are taken from the selected areas from the donor blocks and embedded into the recipient block as an array in pre-determined locations. The resulting TMA block can then be sectioned, and sections mounted onto a microscope slide for various techniques such as IHC. For the study of prognostic biomarkers the tissues from donor blocks need to have associated clinical outcome data. The benefit of TMAs for cancer biomarker analysis is that a large patient cohort with hundreds of cases can all be analysed in parallel with the same experimental conditions (Voduc

et al., 2008). While conducting immunolabelling on single block sections may provide a larger cross sectional area of tissue to analyse biomarkers, a study comparing 0.6 mm diameter TMA cores to their donor blocks found that both had similar ability in the detection of clinically relevant molecules (Sauter, 2010). The utility of TMAs versus immunolabelling from individual tumour blocks is that the IHC immunolabelling conditions are identical between all cores in the TMA which would be difficult to maintain for hundreds of individual tumour slides, thereby avoiding technical variability between cases (Voduc et al., 2008).

***RATIONALE, HYPOTHESIS AND OBJECTIVES***

While the accurate prognostication of many canine MCTs is sufficiently conducted by the current grading schemes and molecular markers, there are a significant subset of MCTs whose biological behaviour remains difficult to predict. Therefore, it is important to identify additional prognostic markers that can be used to predict outcome for both cutaneous/dermal and subcutaneous MCTs. Epigenetic DNA methylation as well as the enzymes involved in methylation and demethylation are often dysregulated in various cancers. Since epigenetic regulation is important in the development and disease progression of myeloid cells including mast cells, dysregulation of epigenetic markers and enzymes could be useful in determining more aggressive canine MCTs.

I therefore hypothesize that 5MC, 5HMC, DNMT1, DNMT3a, TET2, IDH1, and IDH2 global levels may be useful as markers for aggressive canine MCT disease. To test this Hypothesis, the following Objectives are proposed:

*Objective 1:* Validate commercially available antibodies for their ability to recognize canine DNMT1, DNMT3a, TET2, IDH1, and IDH2

*Objective 2:* Optimize immunohistochemistry (IHC) labelling of canine formalin fixed paraffin embedded mast cell tumours for 5MC, 5HMC, DNMT1, DNMT3a, TET2, IDH1, and IDH2 and perform optimized IHC on a tissue microarray of canine MCT

*Objective 3:* Quantify IHC levels using commercially available histopathology image analysis software and determine associations with clinical outcome.

The results of this study will aid in determining whether global expression levels of 5MC, 5HMC, DNMT1/3a, TET2 and IDH1/2 are prognostic markers for canine MCTs.

***METHODS***

SDS-PAGE and Western Blotting

Protein lysates from canine mast cell lines MCT1 (adherent cell line) and MCT2 (suspension cell line), canine B-cell lymphoma cell line CBCL1, and canine kidney MDCK cell line were provided by other researchers (see Declaration of Work Performed for details). Human Liver Whole Tissue Lysate (Adult Whole Normal) NB820-59234 was purchased from Novus Biologicals. Antibodies used for detecting proteins of interest were: DNMT1 (Anti-DNMT1 antibody [EPR18453] ab188453), DNMT3a (Anti-DNMT3a antibody-N-terminal ab228691), IDH1 (abcam Anti-IDH1 antibody [EPR12296] ab172964), and IDH2 (abcam Anti-IDH2 antibody [EPR7577] ab131263).

SDS-PAGE was performed using 30 µg of total protein for MCT1, MCT2, CBCL1, and MDCK cell lysates, and 10 µg total protein for Human Liver Whole Tissue Lysate, all in a total volume of 30 µL/well. Protein lysates were mixed with appropriate volumes of 8X loading buffer and MilliQ water, vortexed and centrifuged, placed on a heating block at 95°C for 5 minutes then vortexed again. Samples were loaded onto a 10% SDS-PAGE gel along with a pre-stained protein ladder (GeneDirex). Electrophoresis was run at 60 V in running buffer (Appendix 1) until the dye front passed the stacking gel, then the voltage was brought up to 120V to complete the electrophoresis. For DNMT3a and TET2, the electrophoresis was continued for additional time after the dye front had run off the gel, to ensure adequate resolution.

A polyvinylidene difluoride (PVDF) membrane (Millipore Sigma) was activated for five minutes in methanol and the gel was equilibrated for five minutes in a transfer buffer solution (Appendix 1). The transfer cassette was prepared by stacking a transfer sponge then a thick

filter paper, the SDS-PAGE gel, the PVDF membrane, and three thin filter paper sheets the same size as the gel and a transfer sponge from bottom to top. The transfer ran at 100 V for 2 hours with the transfer apparatus covered in ice. For TET2 gels, a modified transfer buffer was used (Appendix 1) due to the larger molecular weight of the target protein. The transfer for TET2 gels was performed at 70 V for 3 hours with the transfer apparatus covered in ice. After all transfers, the PVDF membrane was removed and washed with Tris-Buffered Saline-Tween 20 (TBS-T; Appendix 1).

The membranes were then blocked in TBS-T with 5% skim milk powder for 1 hour with rocking at room temperature, then DNMT1, DNMT3a, TET2, IDH1, or IDH2 primary antibodies were added at 1:1000 dilution in blocking solution (Appendix 1). For TET2 detection, a 1:500 dilution in blocking solution was used and membranes were incubated with rocking overnight at 4°C. After transfer, membranes were washed in TBS-T with rocking at room temperature for 15 minutes, three times. Then membrane was incubated with rocking for 1 hour at room temperature with 1:10,000 dilution of goat anti-rabbit secondary antibody (Millipore Sigma) in blocking solution for DNMT3a, DNMT1, IDH1, and IDH2 and with goat anti-mouse secondary antibody (Millipore Sigma) in blocking solution for TET2. Incubation with secondary antibody was followed by another set of three washes for 15 minutes each in TBS-T with rocking at room temperature. The membranes were then placed in clear plastic sheet protectors and their surface was covered with Immobilon Forte (Millipore Sigma). The membranes were then placed in a BioRad ChemiDoc XRS+ and imaged using the colorimetric and chemi function in the ImageLab program. Images were collected just before bands reached oversaturation.

Immunohistochemistry Antibody Immunolabelling

To quantify the staining level of 5MC, 5HMC, DNMT1, DNMT3a, TET2, IDH1, and IDH2 TMAs where immunolabelled and staining was analyzed. Antibodies for 5MC (Millipore Sigma Anti-5-methylcytosine, clone 33D3) and 5HMC (Invitrogen 5-Hydroxymehtylcytosine Monoclonal Antibody (RM236)) were obtained; antibodies for other markers were as described for western blotting. Several optimization procedures were performed to achieve optimal immunolabelling. Details are described in Appendix 2.

A previously prepared Tumour Microarray (TMA) was used for this study (Knight et al., 2021; Thompson, Pearl, et al., 2011). The TMAs were constructed by taking from one to three 0.6 mm diameter core samples, depending on how much area was available of the tumour from the donor block. If there was less than 25 $mm^2$ of tumour available in the donor block, then one or two cores were taken and embedded into the TMA. The TMA contained 244 tumour samples from 189 dogs, distributed with control tissues over two blocks. Clinical outcome data were associated with many of the cases. TMA slides were sectioned at 5 µm thickness and mounted onto SuperFrost+ microscope slides (Fisher) by the Animal Health Laboratory. Slides were deparaffinized in xylene baths for two minutes with three changes of xylene, then rehydrated in 100% isopropanol for two minutes with three changes, then in 70% isopropanol for two minutes. The slides were then rinsed in $dH_2O$ for two minutes. A solution of 10 mM sodium citrate buffer, pH 6.0 antigen retrieval solution (Appendix 1) was used for antigen retrieval for all antibodies except for 5HMC, which used EDTA pH 9.0 (Appendix 1). For antigen retrieval, a Coplin jar containing appropriate buffer was prewarmed in a water bath at 95°C, then slides were added and incubated for an additional 20 minutes at 95°C. The Coplin jars containing

slides were then removed from the water bath and allowed to cool for 20 minutes at room temperature. At this point, for 5MC and 5HMC detection only, the slides were rinsed with $dH_2O$ then slides were incubated for 15 minutes in 3.5M HCl to denature DNA.

All slides were then rinsed twice in $dH_2O$ followed by Tris buffer (Appendix 1) for three minutes each. Hydrophobic barriers were then drawn around the perimeter of the TMA on the slides with a PAP pen (Vector) to keep blocking solutions, antibodies and chromagen detection systems from running off the slides. To deplete endogenous peroxidase enzyme activity, 250 µL of 3% hydrogen peroxide solution (Fisher) was applied to the slides for three minutes, then slides were rinsed with Tris buffer. In a humidity chamber, 250 µL of 1% normal goat serum in PBE (2% EDTA in PBS) was applied for 10 minutes to block non-specific binding of primary antibodies. Then primary antibodies diluted in PBE were added to the slides and incubated at 4°C overnight in the humidity chamber. Dilutions were: 5MC 1 µg/mL, 5HMC 1:2000, DNMT1 1:100, DNMT3a 1:200, IDH1 1:100, IDH2 1:100. TET2 primary antibody incubation occurred for two hours at 37°C with a dilution of 1:50. For negative controls, primary antibodies were omitted and slides underwent incubation with PBE under equivalent conditions. Slides were then rinsed twice in Tris Buffer for five minutes, discarding buffer between rinses. Secondary antibodies were applied to the slides and incubated in a humidity chamber for 30 minutes. Immunolabelling for 5MC and 5HMC utilized the Dako EnVision HRP labelled Dual Link System, DNMT1, DNMT3a, IDH1, and IDH2 utilized the Dako Labelled Polymer-HRP Anti-Rabbit and TET2 utilized Dako EnVision+ System-HRP Labelled Polymer Anti-Mouse. All Dako labelling systems were employed as per manufacturer's protocols. Slides were then rinsed twice in Tris Buffer for 5 minutes, and Abcam DAB substrate Kit was used for immunodetection. Visualization solution

was prepared according to manufacturer's instructions and incubation times with DAB solution were determined by previous optimization (Appendix 2). DAB incubation times were 10 minutes for 5MC, 5HMC, DNMT3a and TET2, 15 minutes for DNMT1, and 6 minutes IDH1 and IDH2. Slides were then rinsed in $dH_2O$, counterstained with Modified Harris hematoxylin (Fisher, SH26), then rinsed in running $dH_2O$. Following this, slides were dipped once in acid alcohol solution (Appendix 1), rinsed in $dH_2O$, dipped in ammonium water solution (Appendix 1) and rinsed in $dH_2O$. Slides were finally dehydrated in 100% isopropanol baths (three times for two minutes each) then in xylene baths (three times for two minutes each) and then a coverslip was applied with cytoseal XYL (Thermo Fisher).

Immunolabelling Software Analysis

Slides were scanned by the Ontario Institute for Cancer Research (OICR) and files were generated in STS format for analysis of immunolabelling on QuPath (0.1.2) open-sourced quantitative pathology software. Aided by the TMA workflow included in the software, TMAs underwent colour deconvolution based on the DAB staining and hematoxylin detection system. First the software analyzed areas of representative DAB, hematoxylin, and background colour to assign RGB values to deconvolute the DAB chromogen staining, hematoxylin counter stain, and background colour on a pixel basis. This allowed the staining to be separated into layers which could be analyzed separately to accurately determine staining of each cell. Then the TMA was de-arrayed and individual cores were identified and a map was applied to relate immunolabelling data generated from QuPath to the clinical data associated with each core. QuPath was trained to identify canine mast cell tumour cells (details in Appendix 3) and then based on the intensity of the DAB staining observed, values were applied to each cell with 0 for

no staining detected, 1 for low, 2 for moderate, and 3 for high intensity staining. These values assigned to each cell were multiplied by the percentage of total cells stained for each value to generate an H-Score which ranged from 0-300, where 0 would be no cells with detected staining in the core to 300 with all 100% of cells in the core given the highest value of 3 for high intensity staining. DAB staining levels were determined for each TMA stained for a given antibody separately, but cores within the same TMA had their intensities ranked on the same scale which was applied to all cores within the same TMA (Appendix 3). Once cores were assigned an H-score, the cores were then individually analyzed to ensure proper cell staining. Cores with artifacts that lead to less than 30% of the core having neoplastic cell representation were eliminated from the analysis, as well as the cores that were lost during IHC and sectioning. Regions of cores that had collagen or presence of edema or other structures that lead to aberrant cell identification were eliminated by manual annotation so as not to affect the H-score calculations. H-scores were linked to the clinical data associated with the cases and results were then analyzed for survival calculations.

Statistical Analysis

The X-tile program (Camp et al., 2004) was used to determine statistically significant cut-points for survival analysis using visual representation of H-scores in a histogram to stratify the H-scores into statistically significant High and Low groups. Using these X-tile cut points, Kaplan-Meier curves were generated and log-rank analysis was performed for disease free interval (DFI) and overall survival (OS) using GraphPad Prism 9. DFI was defined as the time form the date of diagnosis to the local recurrence or metastasis of the MCT, and OS was defined as the time form the date of diagnosis to the time of euthanasia or death due to causes related or

unrelated to MCT, or to the date of last follow up. DFI and OS curves were generated for all cases, as well as for cases stratified by location (dermal vs subcutaneous MCT) and for cases stratified by intermediate graded for Patnaik grade 2 cases, and Kiupel low grade cases. A $p<0.05$ was considered statistically significant for all analysis.

***RESULTS***

Primary Antibody Validation

To validate the antibodies' ability to detect canine DNMT1, DNMT3a, TET2, IDH1, and IDH2 molecular targets, western blots were conducted. DNMT1, DNMT3a, TET2, IDH1 and IDH2 were all detectable in lysates of canine cells (Figures 1 & 2). For DNMT1, the bands were detected between 180 and 245kDa, and the predicted molecular mass of DNMT1 is 183 kDa (Figure 1B). For DNMT3a, a band was detected at approximately 135 kDa, with the predicted molecular mass of DNMT3a of 102 kDa (Figure 1B). For TET2, bands were detected at around 100 and 245 kDa, and the predicted molecular mass for TET2 is 224 kDa (Figure 1C). For IDH1, bands were detected at approximately 48 kDa, and the predicted molecular mass of IDH1 is 47 kDa (Figure 2A). For IDH2, bands were detected between 35 and 48 kDa in canine and human cell lysates, and very faint bands were detected at approximately 63 kDa in human liver cell lysate (Figure 2B). The predicted molecular mass for IDH2 is 50 kDa. Based on these results, these antibodies are validated for detecting the targeted molecules in canine cells therefore they are appropriate to be used for immunolabelling in canine mast cell tumour specimens.

TMA Analysis

After validating the antibodies, the next step was to use immunolabelling to detect 5MC, 5HMC, TET2, DNMT1, DNMT3a, IDH1, and IDH2 on our MCT TMAs. Negative controls were used to evaluate specific binding in FFPE tissues. As can be seen in Figures 3 and 4 the IHC protocols employed were able to eliminate nonspecific binding of the primary and secondary antibodies. This, combined with the western blot validations helps in providing evidence that the immunolabelling is specific.

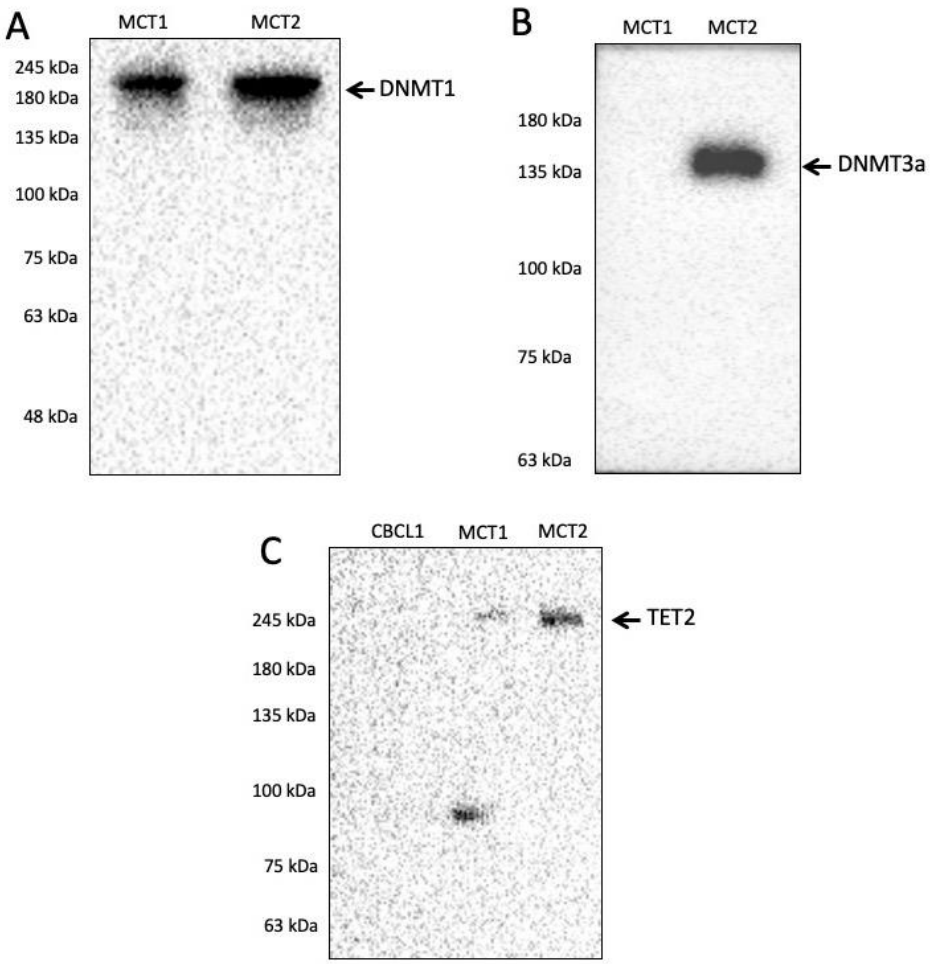


**Figure 1:** Western blots showing validation of antibodies used for immunohistochemistry. DNMT1: predicted molecular mass 183 kDa; DNMT3a: predicted molecular mass 102 kDa; TET2: predicted molecular mass 224 kDa. MCT1, MCT2: canine mast cell cancer cell line lysates; CLBL1: canine B-cell lymphoma cell line lysate. Note that not all samples express detectable levels of these proteins. Note also the lower molecular weight band in panel C, which represents nonspecific binding around 100 kDa in MCT1 cell line lysate.

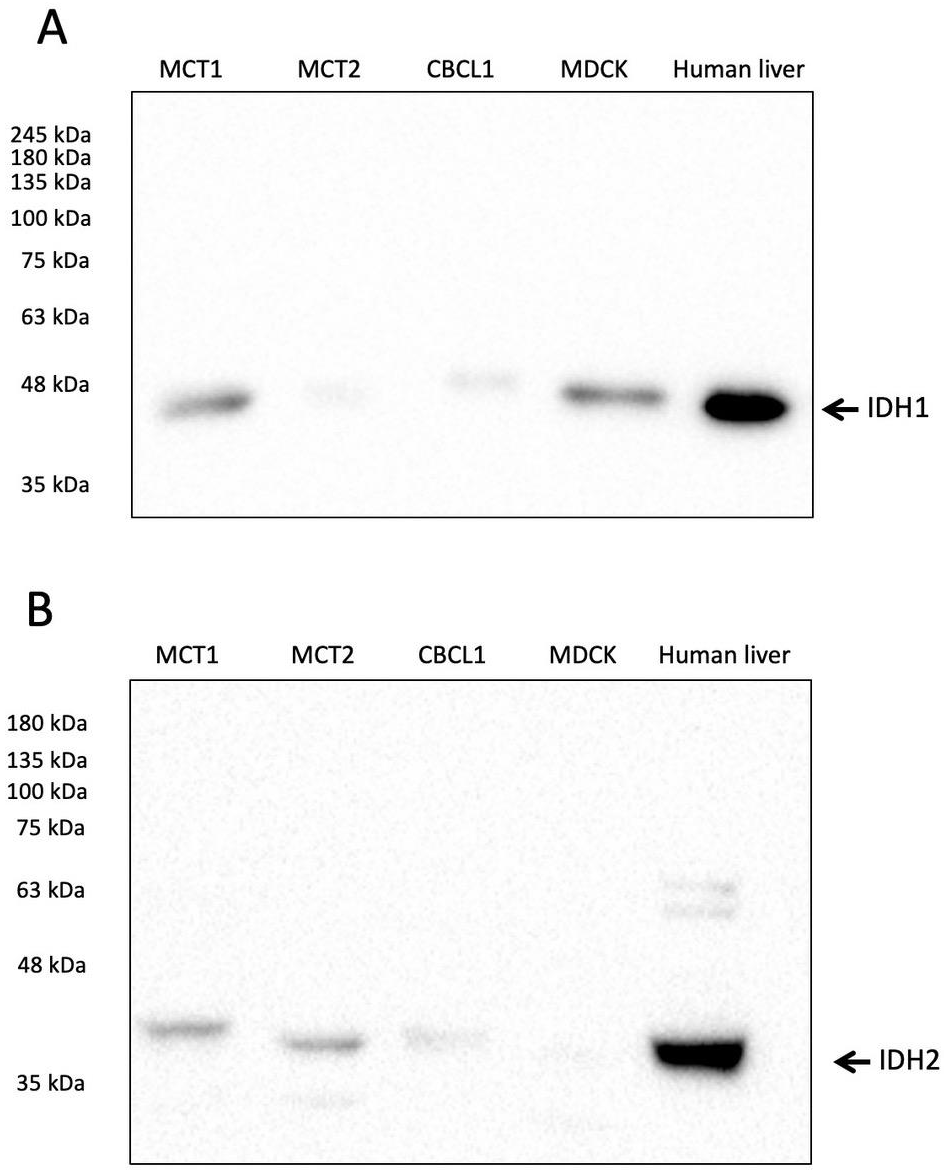


**Figure 2:** Western blots showing validation of antibodies used for immunohistochemistry. IDH1: predicted molecular mass 47 kDa; IDH2: predicted molecular mass 50 kDa. MCT1, MCT2: canine mast cell cancer cell line lysates; CLBL1: canine B-cell lymphoma cell line lysate; MDCK: Madin-Darby canine kidney cell line lysate; Human liver: commercially available lysate for western blotting. Note that not all samples express detectable levels of these proteins.

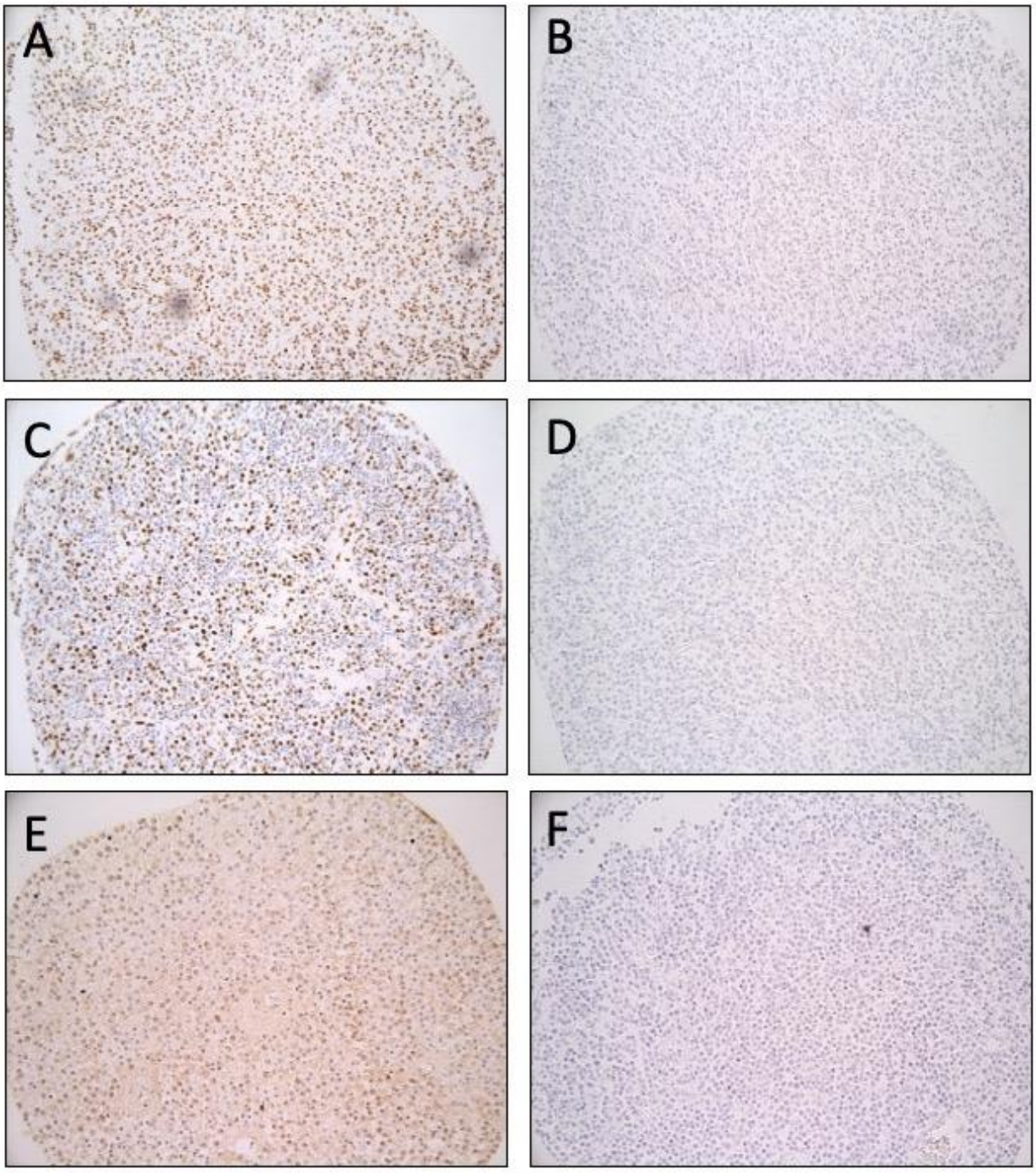


**Figure 3:** Brightfield images of TMA cores after IHC for indicated antigens, showing positive (left column) and negative (right column) immunolabelling. A & B: 5-methylcytosine; C & D: 5-hydroxymethyl cytosine; E & F: TET2. Images taken with 20X objective.

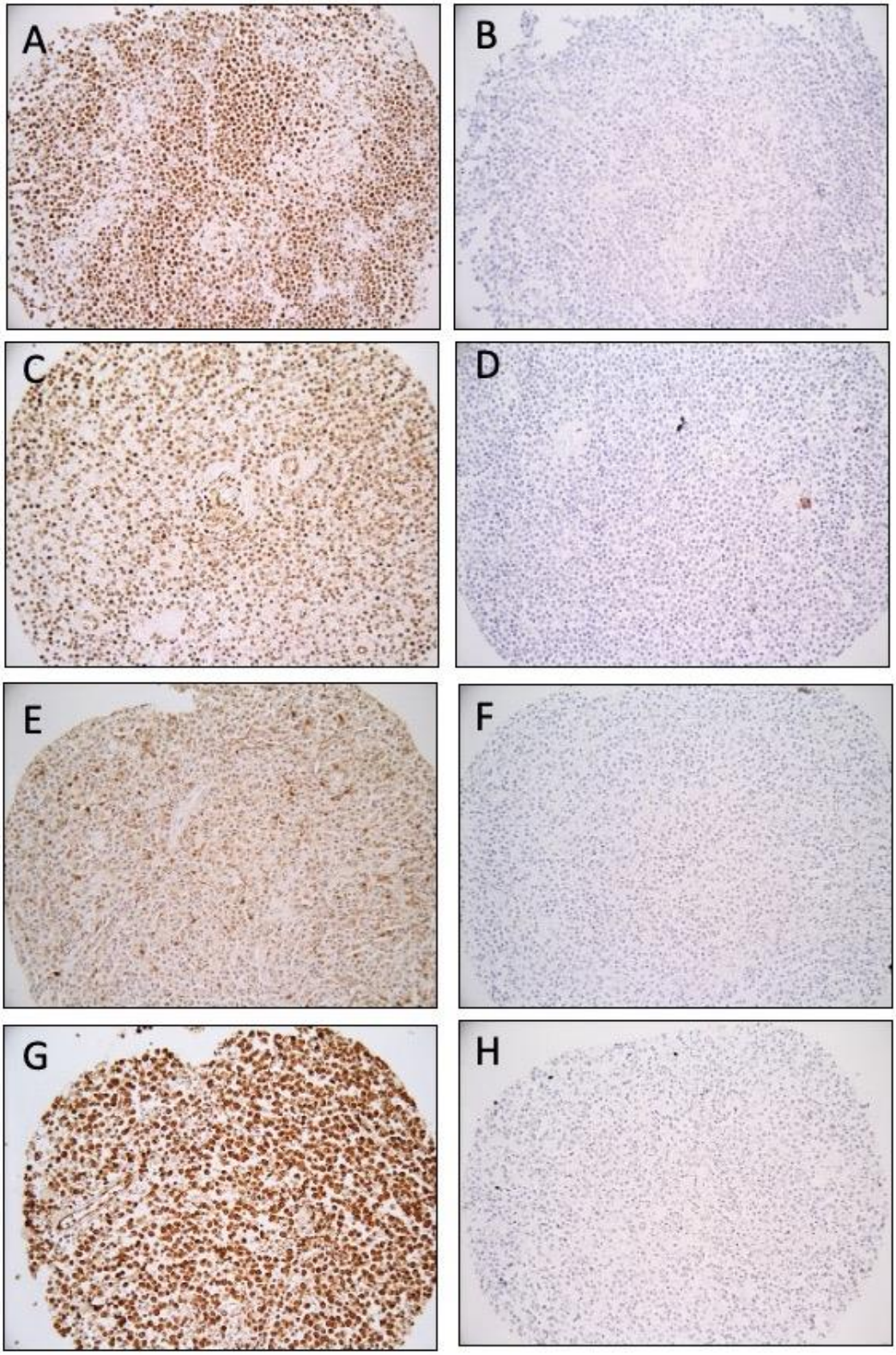


**Figure 4:** Brightfield images of TMA cores after IHC for indicated antigens, showing positive (left column) and negative (right column) immunolabelling. A & B: DNMT1; C & D: DNMT3a; E & F: IDH1; G & H: IDH2. Images taken with 20X objective.

The image of the positively stained TMA was de-arrayed to allow for core mapping, as can be seen in Figure 5A. Cores were then analyzed for staining intensities based on the staining parameters set for the cells. Figure 5B is a screen grab from Qpath software, showing an enlarged image of an individual core. Cells with no staining were given a value of 0 and can be identified by the blue outlines; cells with low staining were given a value of 1+ and can be visualized by the yellow outline; moderate staining was given the value of 2+ and can be visualized by the orange outline, and cells with high staining were given a value of 3+ and can be visualized by the red outline. As can be seen in the red box on the left in Figure 5B, the number of cells were counted for each of the staining intensities, their proportions in the core were then calculated based on the total number of cells, and the core was given an H-score value (seen in the blue box on the left of Figure 5B). Each core was assigned to a unique ID (as seen in the information panel on the left side of Figure 5B), which corresponded to the specific MCT case the core belongs to. All cores in the TMA were thus analyzed and given an H-score. Figure 6 and 7 show examples of cores with low intensity immunolabelling (low H-scores) on the left and cores with high intensity immunolabelling (high H-scores) on the right. Using the unique case IDs, all the cores taken from each case that meet quality control standards were averaged and a single H-score was given to each case. The H-scores for each case were then entered into the X-tile software with their associated DFI and OS data and cut points were determined for survival analysis. An example can be seen with 5MC data in Figure 8.

A

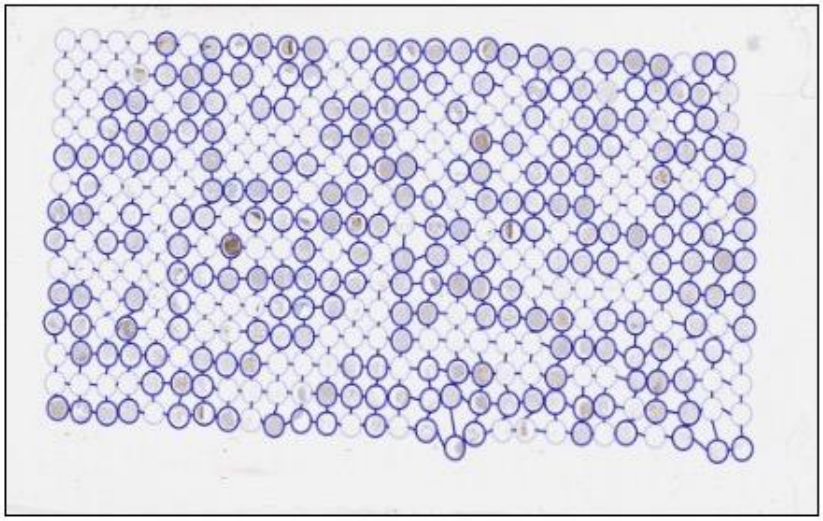

B

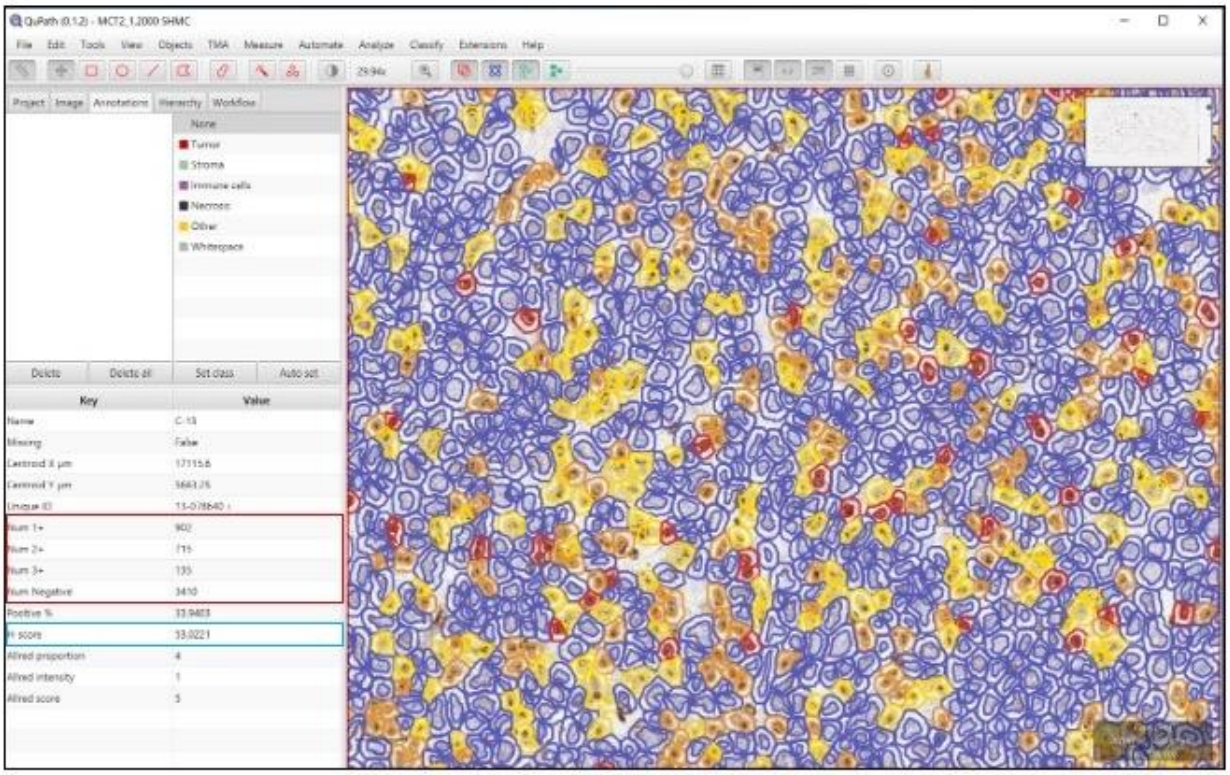


**Figure 5:** Screen shots from Qu-Path analysis. A) An overview of TMA with spot mapping matrix (blue circles). B) A magnified image of an immunolabelled core. The number of cells with staining intensities identified as 1+, 2+, 3+ and negative are outlined in yellow, orange, red and blue, respectively. The area of each category is indicated in the red box on the left, and these values are used to calculate the H-score (blue box on left) for this core.

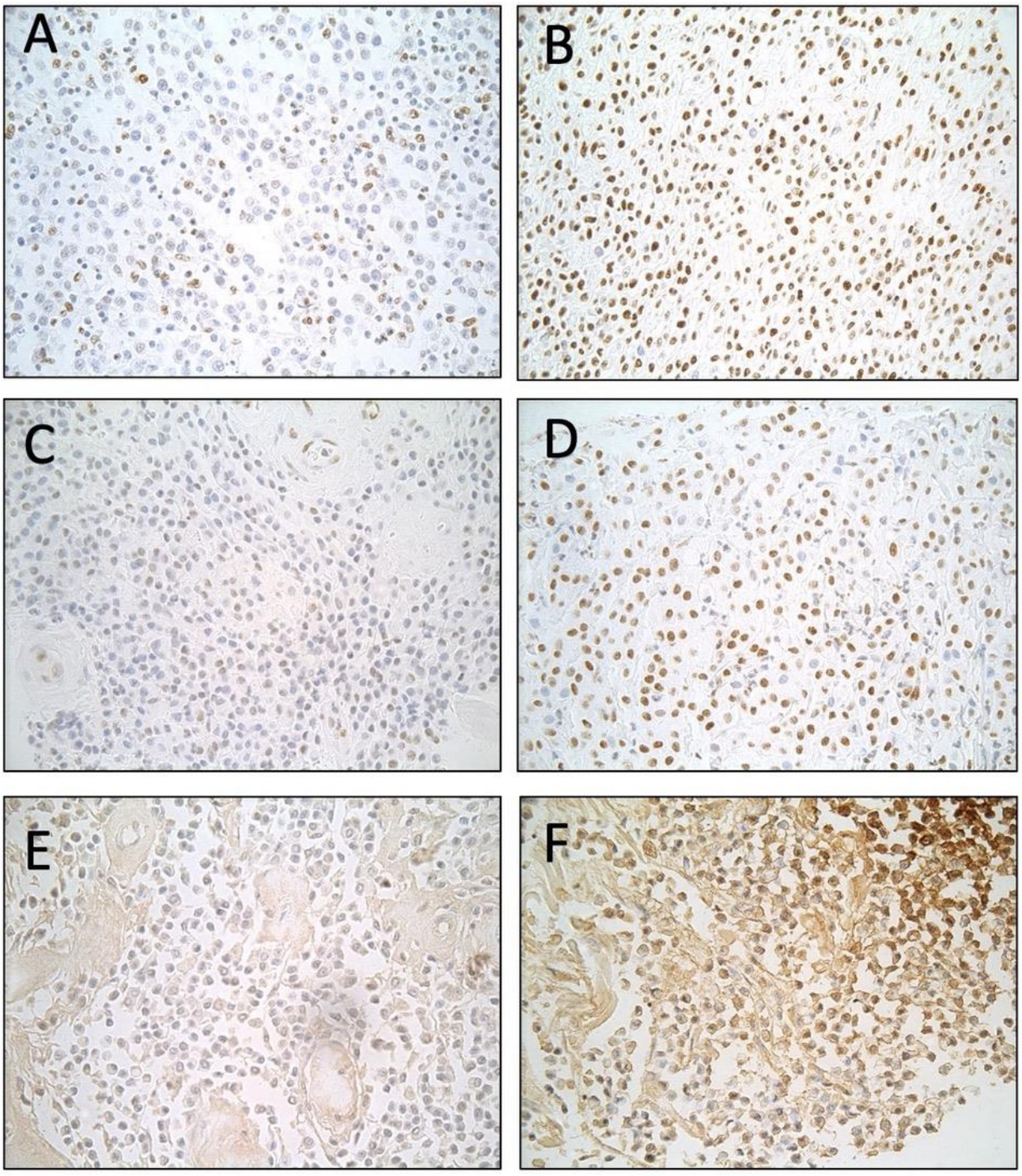


**Figure 6:** Brightfield images of TMA cores after IHC for indicated antigens, showing examples of low H-score (left column) and high H-score (right column) immunolabelling. A & B: 5-methylcytosine; C & D: 5-hydroxymethylcytosine; E & F: TET2. Images taken with 40X objective.

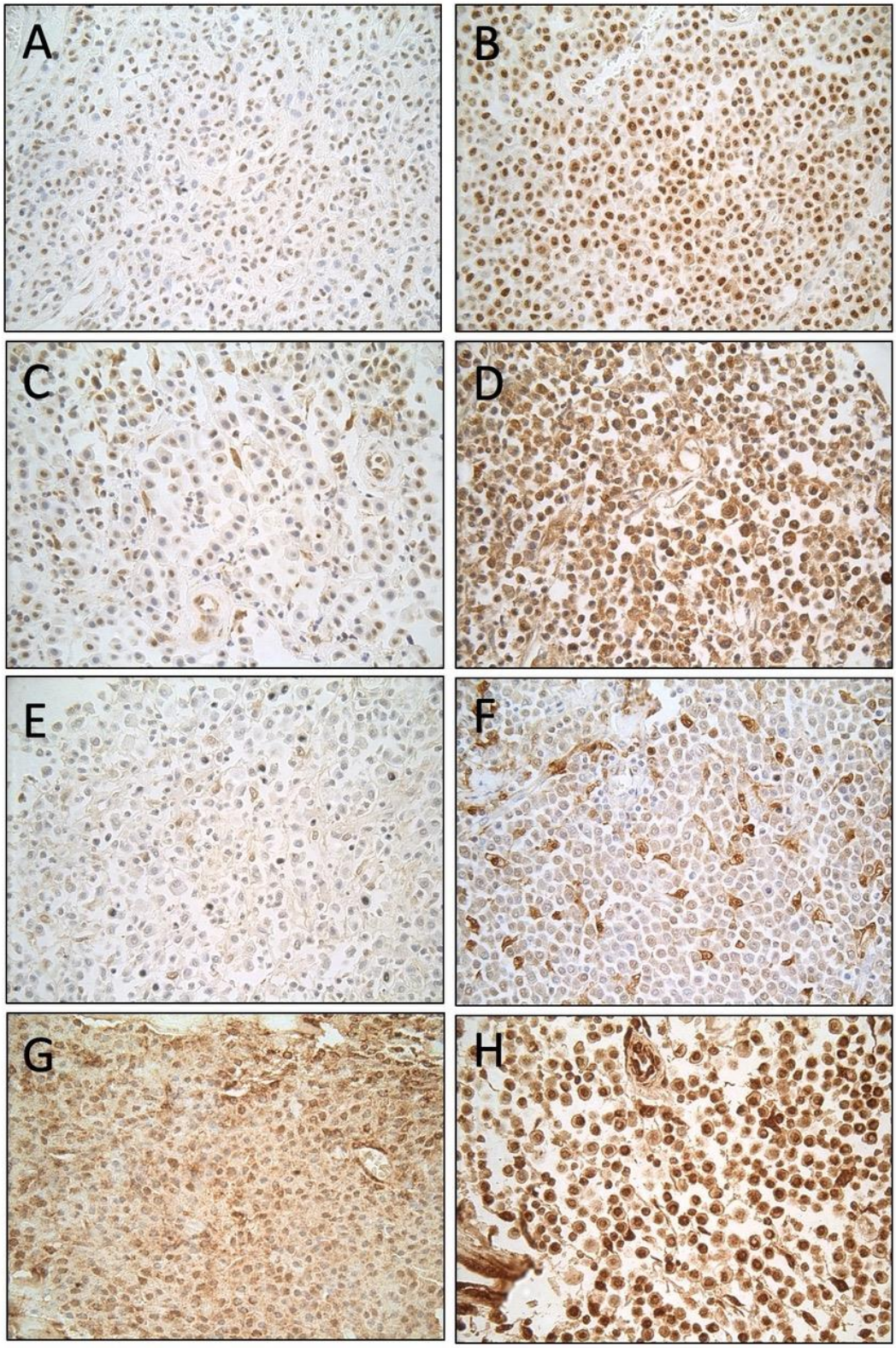


**Figure 7:** Brightfield images of TMA cores after IHC for indicated antigens, showing low H-score (left column) and high H-score (right column) immunolabelling. A & B: DNMT1; C & D: DNMT3a; E & F: IDH1; G & H: IDH2. Images taken with 40X objective.

A

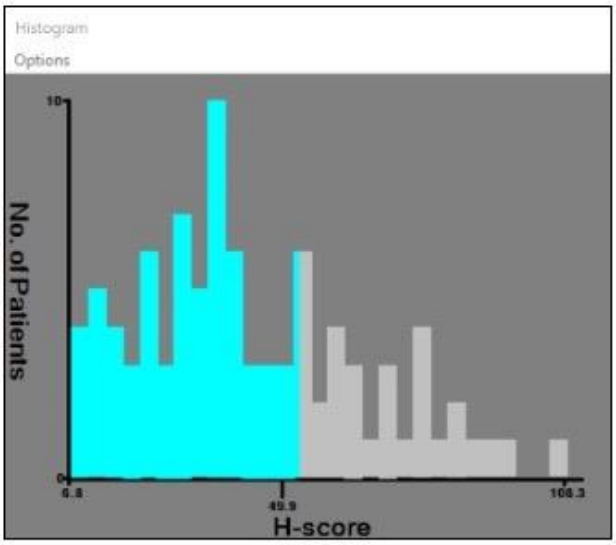


B

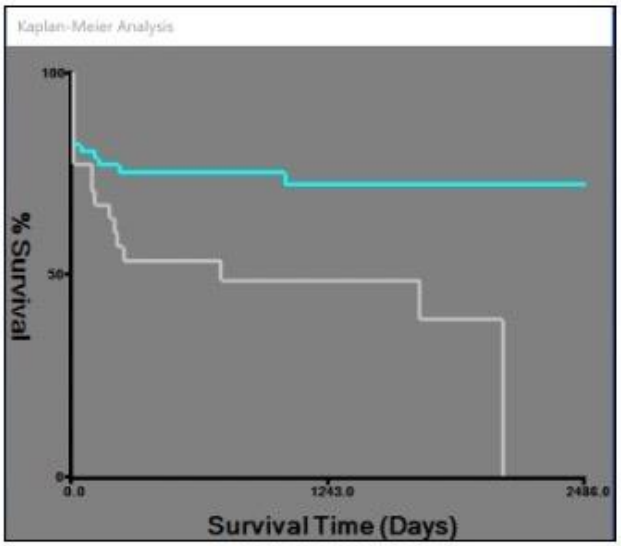


C

| Pt No | % Total | Events | Rate | Rank | Range |
|---|---|---|---|---|---|
| 62 | 66.67 | 16 | 25.81 | 0 to 61 | 6.83 thru 49.91 |
| 31 | 33.33 | 17 | 54.84 | 62 to 92 | 53.70 thru 108.32 |

| | |
|---|---|
| Chi-Square | 6.6580 |
| Uncorrected P | 0.00964 |

**Figure 8:** Outputs from X-tile program for determining cut-point for survival analysis, using 5-methycytosine disease free interval data as an example. A) histogram showing frequency of ranked H-scores. Cursor location is used to divide cases into low (blue) and high (grey) H-scores. B) Kaplan-Meier survival curve based on cursor location shown in (A). C) Numerical readouts for X-tile analysis of this data set.

Outcome Analysis for all Cases of Canine MCT

After accounting for core loss during IHC, and elimination of cores that did not pass the quality control steps, cases with available disease free interval (DFI) and overall survival (OS) data were used for outcome analysis.

For 5MC, 92 cases from the set of all MCTs with outcome information were available for analysis (Figure 9). The difference in DFI between low and high H-scores for 5MC was statistically significant, where cases with low 5MC H-scores were less likely to have recurrence or metastasis (hazard ratio (HR) = 0.42, $p<0.05$) compared to cases with high 5MC H-scores (Figure 9A). For OS, the difference between high and low H-score cases was also statistically significant, where cases with low 5MC H-scores were more likely to not die of compared to cases with high 5MC H-scores (HR = 0.46, $p<0.05$). The median survival time (MST) for low 5MC H-score was 1674 days and for high 5MC H-scores was 577 days. For 5HMC, 89 cases from the set of MCTs with outcome information were available for analysis (Figure 10). There was no significant difference in the DFI ($p >0.1$; Figure 10A) or OS, the MST for low 5HMC H-score was 1671 days, for high 5HMC H-score was 752 days ($p > 0.5$; Figure 10B).

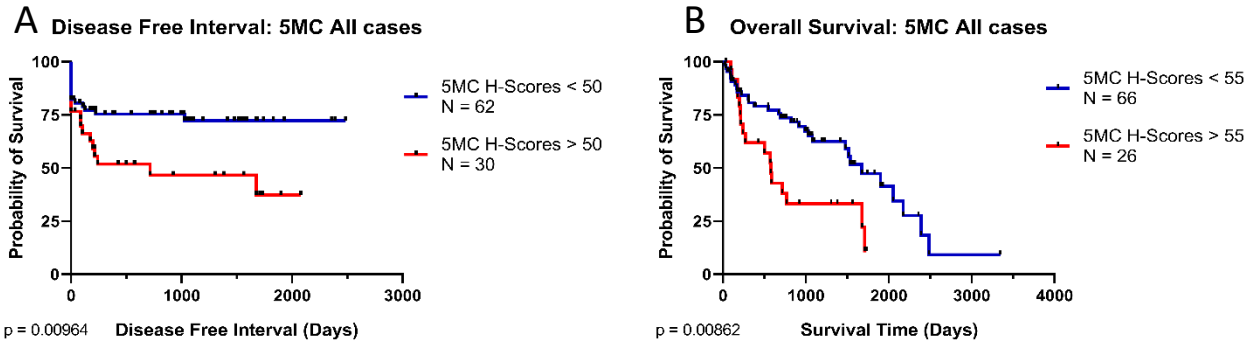


**Figure 9:** Kaplan-Meier survival curves for all mast cell cancer cases stratified by immunolabelling for 5-methylcytosine (5MC). H-scores generated using Qu-Path software were separated based on X-tile analysis into high and low expression. Logrank analysis indicates that cases with low 5MC H-scores (blue) had significantly better Disease Free Interval (A) and Overall Survival (B) compared to cases with high 5MC H-scores (red). Upward ticks indicate censored cases.

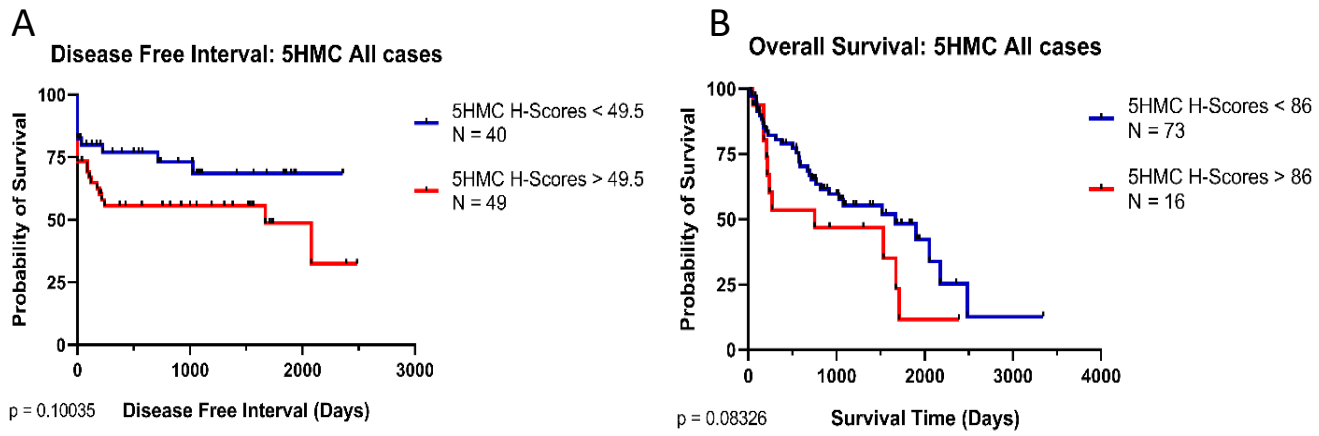


**Figure 10:** Kaplan-Meier survival curves for all mast cell cancer cases stratified by immunolabelling for 5-hydroxymethylcytosine (5HMC). H-scores generated using Qu-Path software were separated based on X-tile analysis into high and low expression. Logrank analysis indicates that there were no significant differences between cases with low 5HMC H-scores (blue) and cases with high 5HMC H-score (red) for either Disease Free Interval (A) or Overall Survival (B). Upward ticks indicate censored cases.

For DNMT1, 112 cases from the set of MCTs with outcome information were available for analysis (Figure 11). The difference in DFI between low and high H-scores for DNMT1 was statistically significant where cases with low DNMT1 H-scores were less likely to have recurrence or metastasis (HR = 0.44, $p<0.05$) compared to cases with high DNMT1 H-scores (Figure 11A). For OS (Figure 11B) the difference between the survival of cases with high and low DNMT1 H-scores was also statistically significant where cases with low DNMT1 scores were more likely to not die compared to cases with high DNMT1 H-scores (HR = 0.48 $p<0.05$). The MST for low DNMT1 H-scores was 1710 days and for high DNMT1 H-scores was 577 days.

For DNMT3a, 90 MCT cases from the set of MCTs with outcome information were available for analysis (Figure 12). The difference in DFI between low and high H-scores for DNMT3a were statistically significant, where cases with low DNMT3a H-scores were less likely to have recurrence or metastasis (HR = 0.44, $p<0.05$) compared to cases with high DNMT3a H-

scores (Figure 12A). For OS (Figure 12B), the difference between the survival of cases with high and low DNMT3a H-scores was also statistically significant, where cases with low DNMT3a scores were more likely to not die compared to cases with high DNMT3a H-scores (HR = 0.34 $p<0.05$). The MST for low DNMT3a H-score was 2079 days and for high DNMT3A H-scores was 88 days.

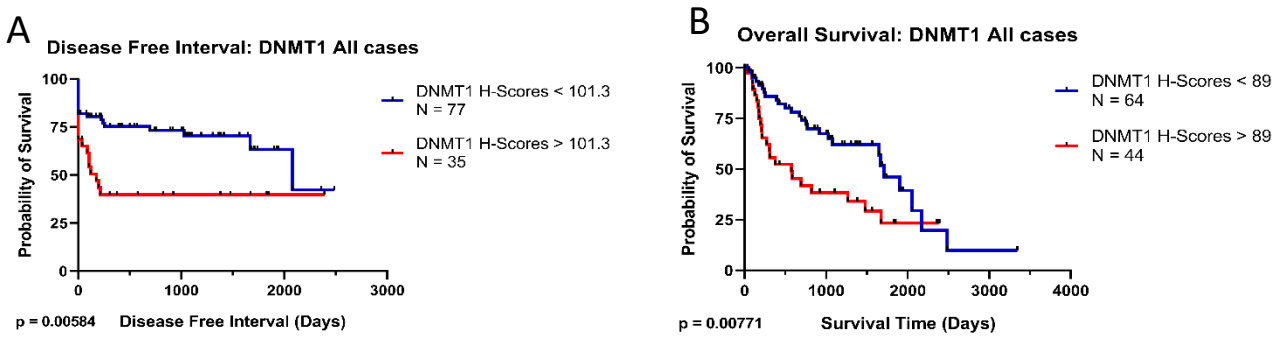


**Figure 11:** Kaplan-Meier survival curves for all mast cell cancer cases stratified by immunolabelling for DNMT1. H-scores generated using Qu-Path software were separated based on X-tile analysis into high and low expression. Logrank analysis indicates that cases with low DNMT1 H-scores (blue) had significantly better Disease Free Interval (A) and Overall Survival (B) compared to cases with high DNMT1 H-scores (red). Upward ticks indicate censored cases.

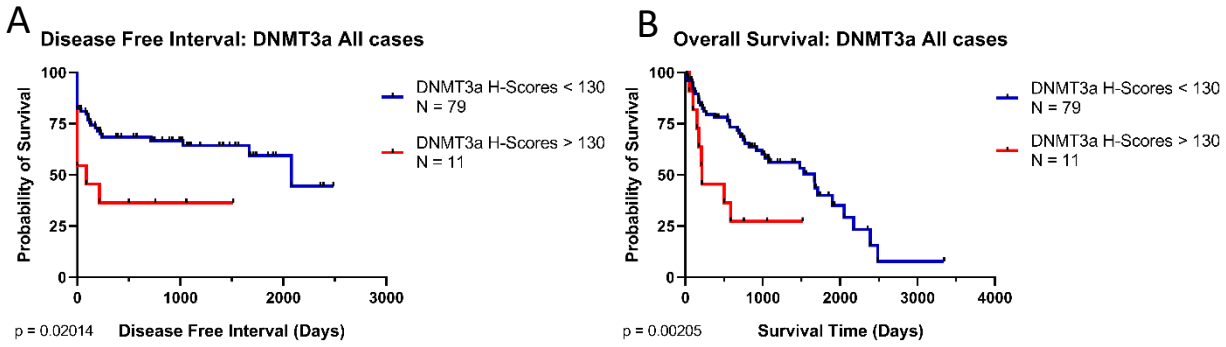


**Figure 12:** Kaplan-Meier survival curves for all mast cell cancer cases stratified by immunolabelling for DNMT3a. H-scores generated using Qu-Path software were separated based on X-tile analysis into high and low expression. Logrank analysis indicates that cases with low DNMT3a H-scores (blue) had significantly better Disease Free Interval (A) and Overall Survival (B) compared to cases with high DNMT3a H-scores (red). Upward ticks indicate censored cases.

For TET2, 81 MCT cases from the set of MCTs with outcome information were available for analysis (Figure 13). The difference in DFI between high and low H-scores for TET2 was statistically significant, where cases with high TET2 H-scores were less likely to have recurrence or metastasis (HR = 0.51, p<0.05) compared to cases with low TET2 H-scores (Figure 13A). For OS (Figure 13B), the difference between the survival of cases with high and low TET2 H-scores was also statistically significant, where cases with high TET2 H-scores were more likely to not die compared to cases with low TET2 H-scores (HR = 0.53 p<0.05). The MST for high TET2 H-score was 1516 days and for low TET2 H-scores was 715 days.

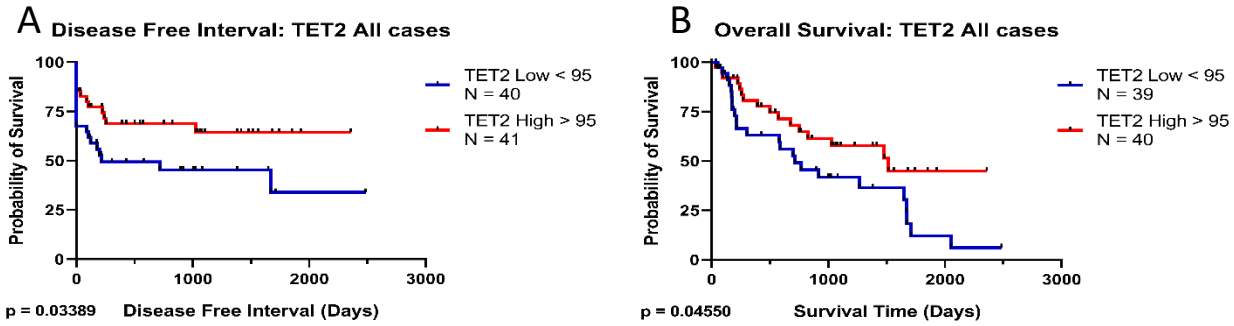


**Figure 13:** Kaplan-Meier survival curves for all mast cell cancer cases stratified by immunolabelling for TET2. H-scores generated using Qu-Path software were separated based on X-tile analysis into high and low expression. Logrank analysis indicates that cases with high TET2 H-scores (red) had significantly better Disease Free Interval (A) and Overall Survival (B) compared to cases with low TET2 H-scores (blue). Upward ticks indicate censored cases.

For IDH1, 71 MCT cases from the set of MCTs with outcome information were available for analysis (Figure 14). The difference in DFI between high and low H-scores for IDH1 was statistically significant, where cases with high IDH1 H-scores were less likely to have recurrence or metastasis (HR = 0.40, p<0.05) compared to cases with low IDH1 H-scores (Figure 14A). For OS (Figure 14B), the difference between the survival of cases with high and low IDH1 H-scores was also statistically significant, where cases with high IDH1 H-scores were more likely to not

die compared to cases with low IDH1 H-scores (HR = 0.41 p<0.05). The MST for high IDH1 H-score was 2054 days and for low IDH1 H-scores was 919 days.

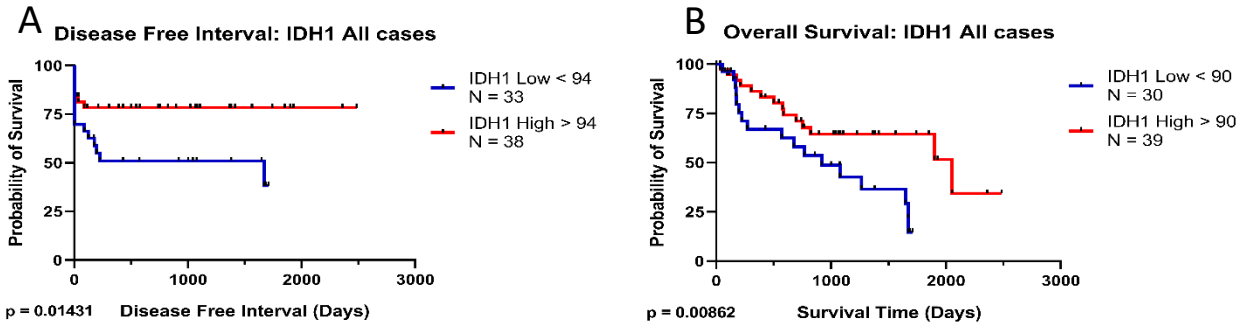


**Figure 14:** Kaplan-Meier survival curves for all mast cell cancer cases stratified by immunolabelling for IDH1. H-scores generated using Qu-Path software were separated based on X-tile analysis into high and low expression. Logrank analysis indicates that cases with high IDH1 H-scores (red) had significantly better Disease Free Interval (A) and Overall Survival (B) compared to cases with low IDH1 H-scores (blue). Upward ticks indicate censored cases.

For IDH2, 80 MCT cases from the set of MCTs with outcome information were available for analysis (Figure 15). The difference in DFI between high and low H-scores for IDH2 was statistically significant, where cases with high IDH2 H-scores were less likely to have recurrence or metastasis (HR = 0.44, p<0.05) compared to cases with low IDH2 H-scores (Figure 15A). For OS (Figure 15B), the difference between the survival of cases with high and low IDH2 H-scores was also statistically significant, where cases with high IDH2 H-scores were more likely to not die compared to cases with low IDH2 H-scores (HR = 0.44 p<0.05). The MST for high IDH2 H-score was 919 days and for low IDH2 H-scores was 239 days.

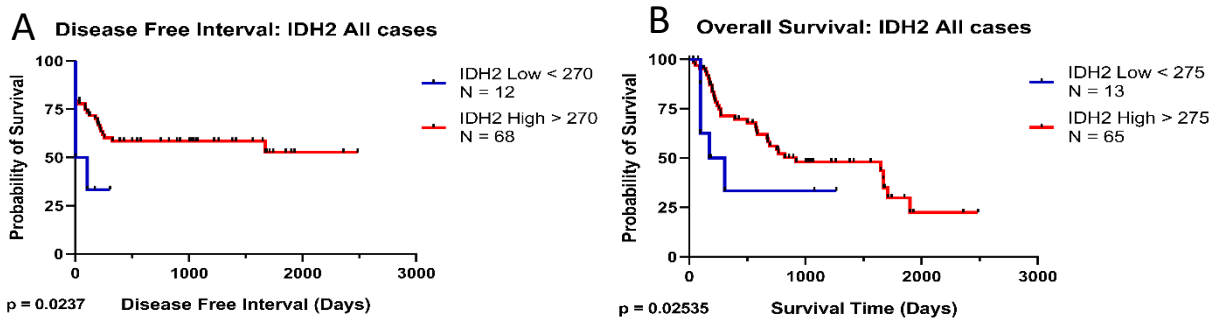


**Figure 15:** Kaplan-Meier survival curves for all mast cell cancer cases stratified by immunolabelling for IDH2. H-scores generated using Qu-Path software were separated based on X-tile analysis into high and low expression. Logrank analysis indicates that cases with high IDH2 H-scores (red) had significantly better Disease Free Interval (A) and Overall Survival (B) compared to cases with low IDH2 H-scores (blue). Upward ticks indicate censored cases.

Disease-Free Interval and Overall Survival for Dermal and Subcutaneous MCTs

Logrank analysis of DFI and OS was conducted for all markers when stratifying the cases by anatomical location of lesion for dermal cases only and subcutaneous cases only. This was conducted to quantify the value of using epigenetic markers to be able to better determine the prognosis of dermal MCTs separate from subcutaneous MCTs due to the differences in their aggressiveness.

For dermal cases only (Table 1), there was no statistically significant difference in the DFI and OS between the high and low H-scores for 5HMC, TET2, IDH1, or IDH2. For 5MC, there was no significant difference in DFI, but for OS the difference between cases with high and low 5MC H-scores was statistically significant, where cases with low 5MC scores were more likely to not die compared to cases with high 5MC H-scores ($p<0.05$). The MST for low 5MC H-score for dermal cases was 1674 days and for high 5MC H-scores was 577 days. For DNMT1, the difference in DFI for low and high H-scores was statistically significant. Cases with low DNMT1 H-scores were less likely to have recurrence or metastasis (HR = 0.2114, $p<0.05$) compared to

cases with high DNMT1 H-scores. For OS, the difference between dermal cases with high and low DNMT1 H-scores was statistically significant, where cases with low DNMT1 scores were more likely to not die compared to cases with high DNMT1 H-scores ($p<0.05$). The MST for low DNMT1 H-score was not reached and for high DNMT1 H-scores was 376 days. When looking at dermal cases immunolabelled for DNMT3a there was no significant difference in DFI, but for OS the difference between dermal cases with high and low DNMT3a H-scores was statistically significant. Cases with low DNMT3a scores were more likely to not die compared to cases with high DNMT3a H-scores ($p<0.05$). The MST for low DNMT3a H-score for dermal cases only was not reached and for high 5MC H-scores was 132 days.

For subcutaneous cases only (Table 2), there were no statistically significant differences in DFI and OS between the high and low H-scores for 5HMC, DNMT1, or DNMT3a. Differences in DFI for low and high 5MC H-scores for subcutaneous cases were statistically significant. Cases with low 5MC H-scores were less likely to have recurrence or metastasis ($HR = 0.2624$, $p<0.05$) compared to cases with high 5MC H-scores. The difference between OS of subcutaneous cases with high and low 5MC H-scores was also statistically significant, where cases with low 5MC scores were more likely to not die compared to cases with high 5MC H-scores ($p<0.05$). The MST for low 5MC H-score was 1535 days and for high 5MC H-scores was 769 days. Differences in DFI for TET2 immunolabelled subcutaneous MCT cases were statistically significant.

**Table 1:** Results of logrank analysis of disease-free interval (DFI) and overall survival (OS) for dermal cases only.

| Marker | Event | N | Log-rank Hazard Ratio | P value |
|---|---|---|---|---|
| 5HMC low | DFI | 21 | 0.4695 | 0.15730 |
| | OS | 20 | 0.6314 | 0.34278 |
| 5MC low | DFI | 18 | 0.5135 | 0.28950 |
| | OS | 25 | 0.3743 | **0.003811*** |
| DNMT1 low | DFI | 39 | 0.2114 | **0.00270*** |
| | OS | 34 | 0.3440 | **0.01141*** |
| DNMT3a low | DFI | 26 | 0.3952 | 0.09426 |
| | OS | 26 | 0.2613 | **0.00336*** |
| TET2 low | DFI | 12 | 1.8380 | 0.29427 |
| | OS | 19 | 2.4350 | 0.09426 |
| IDH1 low | DFI | 16 | 1.5730 | 0.40278 |
| | OS | 16 | 0.6400 | 0.40278 |
| IDH2 low | DFI | 22 | 0.4967 | 0.29427 |
| | OS | 22 | 0.6281 | 0.37109 |

* statistically significantly better outcome for cases with low H-score

Cases with low TET2 H-scores were more likely to have recurrence or metastasis (HR = 2.9160, $p<0.05$) compared to cases with high TET2 H-scores. There was no statistically significant difference between the high and low H-scores of TET2 when looking at subcutaneous MCT cases only. Subcutaneous cases immunolabelled for IDH1 had no significant difference when looking at the DFI, but for OS, the difference between the cases with high and low IDH1 H-scores was statistically significant. Cases with low IDH1 scores were more likely to die compared to cases with high IDH1 H-scores ($p<0.05$). The MST for low IDH1 H-score for subcutaneous cases only was 769 days and for high 5MC H-scores was 2054 days. Likewise, DFI

was not significantly different for subcutaneous cases immunolabelled for IDH2, but for OS the difference between cases with high and low IDH2 H-scores was statistically significant. Cases with low IDH2 scores were more likely to not die compared to cases with high IDH2 H-scores ($p<0.05$). The median survival time (MST) for low IDH2 H-score for subcutaneous cases only was 1710 days and for high 5MC H-scores was 271 days.

**Table 2:** Results of logrank analysis of disease-free interval (DFI) and overall survival (OS) for subcutaneous cases only.

| Marker | Event | N | Log-rank Hazard Ratio | P value |
|---|---|---|---|---|
| 5HMC low | DFI | 25 | 0.6373 | 0.31370 |
| | OS | 37 | 0.4169 | 0.08326 |
| 5MC low | DFI | 33 | 0.2624 | **0.00443*** |
| | OS | 32 | 0.4336 | **0.04042*** |
| DNMT1 low | DFI | 27 | 0.4772 | 0.06928 |
| | OS | 33 | 0.4171 | 0.08326 |
| DNMT3a low | DFI | 24 | 0.6372 | 0.31731 |
| | OS | 25 | 1.2690 | 0.58388 |
| TET2 low | DFI | 8 | 2.9160 | **0.01603¶** |
| | OS | 17 | 2.1370 | 0.09426 |
| IDH1 low | DFI | 9 | 2.4560 | 0.15730 |
| | OS | 9 | 3.6160 | **0.01352¶** |
| IDH2 low | DFI | 11 | 2.0170 | 0.10686 |
| | OS | 27 | 0.3735 | **0.03811*** |

* statistically significantly better outcome for cases with low H-score
¶ statistically significantly better outcome for cases with high H-score

Disease-Free Interval and Overall Survival for Canine MCTS by Grade

Prognostication of canine MCTs given an intermediate grade can have highly variable outcome. To evaluate whether the markers in my study are better able to determine outcome for such cases, logrank analysis of DFI and OS was conducted for all of the markers (5HMC, 5MC, DNMT1, DNMT3a, TET2, IDH1, and IDH2) when stratifying the cases by either Patnaik grade 2 or Kiupel low grade.

Table 3 shows the results of evaluating DFI and OS of Patnaik grade 2 cases only. There were no statistically significant differences in the DFI and OS between the high and low H-scores of Patnaik grade 2 MCT cases immunolabelled for 5HMC, TET2, and IDH2. For Patnaik grade 2 cases immunolabelled for 5MC there was no significant difference in DFI but for OS, the difference between cases with high and low 5MC H-scores was statistically significant. Cases with low 5MC scores were more likely to not die compared to cases with high 5MC H-scores ($p<0.05$). The MST for low 5MC H-score for Patnaik grade 2 cases only was 1674 days and for high 5MC H-scores was 577 days. For DNMT1 and DNMT3a, in both cases there were significant differences in DFI, but not OS for Patnaik grade 2 cases. For DNMT1, cases with low DNMT1 H-scores were less likely to have recurrence or metastasis ($p<0.05$) compared to cases with high DNMT1 H-scores and likewise for DNMT3a ($p<0.05$). For IDH1, Patnaik Grade 2 MCT cases difference in DFI was statistically significant. However, in this analysis, cases with low DNMT1 H-scores were *more* likely to have recurrence or metastasis ($p<0.05$) compared to cases with high DNMT1 H-scores. It is important to note, however, that for all of the Patnaik grade 2 analyses, there were fewer than 5 progression events in the DFI groups, thus this analysis is probably lacking in statistical power.

Table 4 shows the outcome of survival analysis of Kiupel Low Grade cases only. There were no statistically significant differences in DFI or OS between the high and low H-scores of Kiupel Low Grade cases stained for 5HMC, DNMT3a, or TET2. Differences between H-scores for 5MC were statistically significant for both DFI and OS. Cases with low 5MC H-scores were less likely to have recurrence or metastasis ($p<0.05$) and were more likely to not die ($p<0.05$) compared to cases with high 5MC H-scores. ($p<0.05$). The MST for low 5MC H-score

**Table 3:** Results of logrank analysis of disease-free interval (DFI) and overall survival (OS) for Patnaik Grade 2 cases only.

| **Marker** | **Event** | **N** | **Log-rank Hazard Ratio** | **P value** |
|---|---|---|---|---|
| 5HMC low | DFI† | 13 | 0.2598 | 0.06950 |
| | OS | 15 | 0.4094 | 0.14320 |
| 5MC low | DFI† | 14 | 0.7194 | 0.65080 |
| | OS | 16 | 0.2451 | **0.01150*** |
| DNMT1 low | DFI† | 23 | 0.2015 | **0.02014*** |
| | OS | 21 | 0.5638 | 0.31731 |
| DNMT3a low | DFI† | 16 | 0.2371 | **0.02180*** |
| | OS | 14 | 0.4952 | 0.24040 |
| TET2 low | DFI† | 9 | 1.3050 | 0.75183 |
| | OS | 10 | 1.9440 | 0.25421 |
| IDH1 low | DFI† | 6 | 4.5480 | **0.04550¶** |
| | OS | 11 | 1.3810 | 0.58388 |
| IDH2 low | DFI† | 12 | 1.0320 | 1.00000 |
| | OS | 11 | 0.8487 | 0.75183 |

† fewer than 5 events/group

* statistically significantly better outcome for cases with low H-score

¶ statistically significantly better outcome for cases with high H-score

was 2054 days and for high 5MC H-scores was 992 days. When looking at Kiupel Low Grade cases immunolabelled for DNMT1 there was no significant difference in DFI but the difference between the OS of cases with high and low DNMT1 H-scores was statistically significant. Cases with low DNMT1 H-scores were more likely to die compared to cases with high DNMT1 H-scores ($p<0.05$). The MST for low DNMT1 H-score for Kiupel Low Grade cases only was 1027 days and for high DNMT1H-scores was 2054 days. For both IDH1 and IDH2, similar outcomes were seen with survival analysis of Kiupel Low Grade cases. While differences in H-score did not lead to statistically significant DFI, OS was significantly associated with IDH1 or IDH2 H-score. Cases with low IDH1 H-scores were more likely to die compared to cases with high IDH1 H-scores ($p<0.05$). The MST for low IDH1 H-score for Kiupel Low Grade cases only was 919 days and for high IDH1H-scores was 2054 days. Likewise, cases with low IDH2 H-scores were also more likely to die compared to cases with high IDH2 H-scores ($p<0.05$). The MST for low IDH2 H-score for Kiupel Low Grade cases only was 919 days and for high IDH2H-scores was not reached.

**Table 4:** Results of logrank analysis of disease-free interval (DFI) and overall survival (OS) for Kiupel Low Grade cases only.

| Marker | Event | N | Log-rank Hazard Ratio | P value |
|---|---|---|---|---|
| 5HMC low | DFI | 19 | 1.6700 | 0.52709 |
| | OS | 19 | 0.8635 | 0.52709 |
| 5MC low | DFI | 49 | 0.3019 | **0.01079*** |
| | OS | 46 | 0.4512 | **0.04288*** |
| DNMT1 low | DFI | 57 | 0.5383 | 0.25421 |
| | OS | 14 | 2.4680 | **0.02811¶** |
| DNMT3a low | DFI | 34 | 0.6334 | 0.31731 |
| | OS | 10 | 1.3210 | 0.27332 |
| TET2 low | DFI | 22 | 2.0260 | 0.19229 |
| | OS | 24 | 1.6010 | 0.29427 |
| IDH1 low | DFI† | 16 | 2.0350 | 0.54881 |
| | OS | 13 | 4.4340 | **0.00165¶** |
| IDH2 low | DFI | 19 | 1.8460 | 0.25421 |
| | OS | 22 | 2.9820 | **0.03594¶** |

† fewer than 5 events/group

* statistically significantly better outcome for cases with low H-score

¶ statistically significantly better outcome for cases with high H-score

***DISCUSSION***

Mast cell tumours are a very common neoplasm that occurs in dogs, consisting of up to 21% of all canine skin tumours (Garrett, 2014). While grading of these MCTs with the Kiupel and Patnaik systems are considered the gold-standard for MCT prognosis, there is a wide variability in the biological behavior of low grade MCTs (Garrett, 2014; Kiupel et al., 2011). Hence there is a need for other ways to prognosticate aggressive MCT disease. As there is often a dysregulation in DNA methylation of hematologic cancers such as acute myeloid leukemia (AML) it is possible that there are dysregulations in the methylation marks and methylation and demethylation enzymes in MCTs as well (Dexheimer et al., 2017). This study was therefore done to identify if there was an association between the levels of 5MC, 5HMC, DNMT1, DNMT3a, TET2, IDH1, and IDH2 and canine MCT outcome, and if the levels of these biomarkers could be prognostic. High 5MC levels were associated with poorer DFI and/or OS in canine MCTs and high 5MC levels showed significance for poorer DFI and OS when stratifying the cases by dermal and subcutaneous tissue location and in intermediately graded cases. High levels of DNMTs and low levels of TET2 and IDHs showed significance for poorer DFI and OS in MCTs as well. When stratifying by location, high levels of 5MC and DNMTs showed poorer DFI and OS in dermal cases while in subcutaneous tissues high levels of 5MC and low levels of TET2 and IDHs were associated with poorer DFI and OS. For intermediately graded tumours high levels of 5MC and DNMTs and low levels of IDHs were associated with poorer DFI and OS. Therefore, there is potential for these markers not only to predict more aggressive behavior but to identify aggressive cases based on location as well as in intermediately graded MCTs.

DNMT enzymes covalently add a methyl group onto the 5' carbon of cytosine. This modification is referred to as 5-methylcytosine (5MC), while 5-hydroxymethylcytosine (5HMC) is the product of oxidation of 5MC by the TET enzymes (L. I. Kroeze et al., 2015; Meng et al., 2015). In my study, cases with overall levels of 5MC staining with a higher overall H-score showed poorer overall survival (OS) and worse disease free interval (DFI) compared to cases with lower H-scores. A previous study conducted by Morimoto *et al*. found that MCT cases that showed global hypomethylation were associated with Patnaik grade 3 and Kiupel high grade (Morimoto *et al*., 2017). That study did not evaluate case outcome. However, by comparing the 5MC immunolabelling intensity based on Patnaik and Kiupel grade in my study I found no significant difference by either grading scheme grade for both 5MC and 5HMC in my cases (Appendix 4). When looking at the overall levels of 5HMC there was also no significant difference in the high and low H-score immunolabelling intensity when comparing all groups or when stratifying the cases by lesion location. High levels of 5MC (*i.e.* hypermethylation) was associated with poorer OS when looking at all cases and locations, as well as poorer DFI when looking at all cases and subcutaneous MCT cases in my study.

DNA methylation can be upregulated or downregulated in various cancers as well as within a particular cancer (Bronzini et al., 2017). When measuring the global levels in canine acute myeloid leukemia (AML), Bronzini *et al*. found that the methylation profile was very heterozygous compared to normal samples (Bronzini *et al*., 2017). While neither hypermethylation nor hypomethylation alone was consistently associated with canine AML, there was both global hypermethylation in some cases and hypomethylation in others compared to normal samples (Bronzini et al*., 2017)*. In my study, high 5MC levels were

associated with poorer outcome even when comparing dermal MCT to subcutaneous cases, which tend to be less aggressive and have better prognosis (Thompson, Pearl, et al., 2011). High levels of 5MC were associated with poorer OS for both dermal and subcutaneous MCTs and with poorer DFI in dermal cases. In a study of human AML, Qu *et al*. found that a large component of differentially methylated regions (DMR) were hypermethylated in high risk cytogenic groups versus low and intermediate risk groups, therefore they were able to determine prognosis from methylation levels (Qu et al., 2015). Being able to differentiate the cases that are histologically nonaggressive but biologically aggressive using methylation markers is important to ensure proper treatment options in MCTs. In this study when looking at 5MC levels in intermediate grade MCTs, I found that higher 5MC levels had poorer DFI and OS in Kiupel low grade cases, and poorer OS in Patnaik grade 2 cases. High 5MC levels may therefore be helpful in identifying more biologically aggressive MCT cases, and can aid in prognosis.

DNMT1 is referred to as the maintenance DNA methyltransferase and reestablishes lost methylation markers after DNA replication. DNMT3a is a de novo DNA methyltransferase and it serves to establish new DNA methylation marks (Tajima et al., 2016). DNMTs are often mutated in various hematologic malignancies including various myeloid malignancies (Dexheimer et al., 2017). Mutations in DNMT1 and DNMT3a led to hypermethylation of promoter regions of various tumor suppressor genes such as *p15* and contribute to disease progression in human AML (Wong et al., 2019). While mutational status was not looked at in my study, the global enzyme expression of the maintenance methylator DNMT1 and the de novo methylator DNMT3a were evaluated, and differences in canine MCT outcome were

associated with different DNMT H-scores. Mizuno *et al*. found that both DNMT1 and DNMT3a were overexpressed in human AML compared to normal cells, and that these upregulations were associated with hypermethylation of tumor suppressor genes associated with progression such as *p15* (Mizuno *et al*., 2001). It would be interesting to evaluate hypermethylation of similar tumour suppressor genes in canine MCT, and see if it associates with DNMT expression patterns.

Overexpression of DNMTs is seen in other cancers as well. In head and neck squamous cell carcinoma (HNSCC) there was an increase in the transcription level of DNMT1 (Cui et al., 2021). Immunolabelled HNSCC tissues with increased DNMT1 expression were associated with higher pathological grade (Cui *et al*., 2021*)*. In my study, high levels of DNMT1 and DNMT3a expression were associated with poorer DFI and OS in all cases. When stratifying MCT cases based on lesion location, increased levels of DNMT1 were associated with poorer DFI and OS, and high DNMT3a levels were associated with shorter OS. When stratifying MCT cases by grade, high levels of DNMTs were associated with poorer DFI in Patnaik grade 2 cases, however there were too few cases for high and low H-scores when looking at DFI for Patnaik grade 2 cases for DNMT1. Mutations in DNMTs lead to hypermethylation in various cancers and since my study found an increase in 5MC immunolabelling in these MCTs then the increase in DNMTs could potentially explain this upregulation and could have significance in prognosis of dermal MCTs. In support of this, I found a significant positive correlation between 5MC and DNMT3a (but not DNMT1) levels in my MCT cases (Appendix 4).

TET enzymes are responsible for the oxidation of 5MC into 5HMC as well as the subsequent oxidations during the process of DNA demethylation (L. I. Kroeze et al., 2015). In

this study low immunolabelling of TET2 levels in canine MCT cases was associated with a poorer DFI and shorter OS. TET2 is often dysregulated in hematopoietic cancers and De Vita *et al*. showed that a loss of TET2 leads to impaired differentiation and increased proliferation of mature mast cells in mice (De Vita e*t al*., 2014). TET2 is often mutated in human myeloid malignancies such as AML and myelodysplastic syndrome (MDS) (Scopim-Ribeiro *et al*., 2015). Scopim-Ribeiro *et al*. found AML and MDS had low expression of TET2 compared to normal cells and these lower levels were associated with worse event free survival and OS (Scopim-Ribeiro *et al*., 2015). In a study conducted by Zhang *et al*. TET2 expression levels were independently prognostic in CN-AML patients and low levels of TET2 enzyme expression were associated with shorter OS (Zhang et al., 2018). They also found that when analyzing a cohort of patients from The Cancer Genome Atlas (TCGA), TET2 expression levels were not associated with TET2 mutations in AML. This suggests that regardless of mutation status, low TET2 expression was prognostic in CN-AML (Zhang *et al*., 2018). In my study, low TET2 immunolabelling was associated with shorter DFI in subcutaneous but not in dermal MCTs.

Normal IDH1/2 function is to catalyze the oxidative decarboxylation of isocitrate to $\alpha$-ketoglutarate in the tricarboxylic acid cycle and $\alpha$-ketoglutarate along with Fe(II) is an important cofactor in normal TET2 enzyme function (Huang & Rao, 2014). When mutated, IDH1/2 often further convert $\alpha$-ketoglutarate into D-2HG which acts as an agonist for TET2 and along with reducing the supply of $\alpha$-ketoglutarate inhibits normal TET2 function (Figueroa et al., 2010; Huang & Rao, 2014). Immunolabelling levels of IDH1 and IDH2 were also evaluated in my study, and for both the enzymes lower immunolabelling levels were associated with poorer DFI and shorter OS when looking at all MCT cases. Figueroa *et al*. looked at IDH1 and IDH2

mutations in human AML cells and found mutant cells had an increased global methylation status compared to normal CD34+ bone marrow cells. They proposed this was due to increased D-2HG levels in mutant cells (Figueroa *et al*., 2010). IDH mutated AML cells actively inhibited the functions of TET2 enzymes through these increased levels of D-2HG function leading to an increase in global 5MC levels (Figueroa et al., 2010). They also found that AML patient samples with IDH1/2 mutations had significant hypermethylation compared to normal bone marrow samples taken from healthy patients and reported 154 hypermethylated genes of which a majority had more than 2-fold decrease in expression (Figueroa et al., 2010).

IDH mutations in an in vivo disease model of gliomas led to disease progression (Turcan *et a*l., 2013). The associated upregulated D-2HG led to global hypermethylation, establishing a phenotype in gliomas called glioma CpG island methylator phenotype (Turcan *et al*., 2013). However, mutation status of IDH enzymes was not looked at in this study and nor were levels of D-2HG, which would have determined if there was a gain of function mutation in the IDHs. Figueroa *et al*. also found that AML cases with TET2 mutations and IDH mutations both showed similar hypermethylated patterns, however IDH mutations were associated with a greater amount of promoter hypermethylation and global hypermethylation. In my study, low levels of IDH1 or IDH2 were associated with shorter OS in subcutaneous and in Kiupel low grade cases. Therefore, dysregulation of IDHs and TETs could be prognostic in subcutaneous MCTs since low levels were associated with poorer DFI and OS in subcutaneous MCTs and an increase in 5MC levels, similar to observations in the previously mentioned studies. This was separate to what was observed in dermal cases, where increased levels of DNMTs were associated with poorer DFI and OS in dermal cases and also showed an increase in 5MC levels. This suggests that while

DNA hypermethylation was indicative of poor prognosis in all MCT cases, levels of IDHs and TET2, and levels of DNMTs have significant impact on outcome in subcutaneous and dermal cases, respectively.

Other studies have associated IDH, TET and DNMT dysregulation with increases in global levels of DNA methylation (Figueroa et al., 2010; Ma et al., 2018; Turcan et al., 2013). This, coupled with the findings of my study suggest that the increased levels of 5MC in any MCT case, as well as increased DNMT levels in dermal cases and decreased levels of TET2 and IDHs in subcutaneous cases may be prognostic markers for response to treatments with hypomethylating agents such as 5-aza2-deoxycytidine (Decitabine) and 5-azacytidine (Azacitidine). Decitabine and Azacitidine work by becoming cytidine analogs when incorporated in DNA and RNA respectively (Derissen et al., 2013). In low doses they form adducts between DNMTs and DNA which are then degraded by proteosomes, allowing DNA synthesis to resume in the absence of DNMTs thereby reducing methylation (Derissen et al., 2013). In a study by Bejar *et al*. they found that human myelodysplastic syndrome (MDS) cases with TET2 mutations predicted an increased response to both Decitabine and Azacitidine (Bejar *et al*., 2014). They also looked at mouse models, and those with TET2 loss and increased myeloid progenitor proliferation were more sensitive to Azacytidine (Bejar *et al*., 2014). Since the low levels of TET2 were associated with poorer DFI and OS in human MDS, perhaps low levels of TET2 expression in canine MCTs could identify cases that would be more sensitive to hypomethylating agents. Traina *et al*. also found that TET2 mutations in MDS were predictive of better overall response rates to treatments with Azacitidine and Decitabine (Traina et al., 2014). Further, they reported that MDS cases with mutant DNMT3a expression also showed better overall response rates to

the hypomethylating agents (Traina et al., 2014). Therefore, increased levels of DNMTs, specifically DNMT3a, could determine canine MCT cases that would respond well to such hypomethylating agents.

Immunohistochemistry (IHC) was conducted for each of the antibodies on the MCT TMA. There are various pitfalls that can occur during the IHC process that can alter results, therefore careful optimization is needed to ensure validated results (Kim et al., 2016). One of the major issues with IHC is to ensure that the antibodies are able to identify the target antigen in the tissue of interest. One method to validate antibody specificity is by western blot. Ensuring the primary antibody of interest can detect a single band at the correct molecular weight in the target cells helps in confirming antibody specificity (Janardhan et al., 2018). As the antibodies used for my study were not developed for canine tissue, validation was necessary to confirm detection of the relevant enzymes in canine cells. To address this issue a western blot was conducted for each of the antibodies for the DNMT1, DNMT3a, TET2, IDH1, and IDH2 enzymes using cell lysates from two canine MCT cell lines (MCT1 and MCT2), a canine B-cell lymphoma cell line (CBCL1), Madin-Darby canine kidney cell line (MDCK), and a commercially available human liver lysate for western blotting. To ensure that the antibodies were able to detect the target enzyme in canine cells the validation of the antibodies was important. Non-specific binding of the TET2 antibody (which has been reported in the datasheet for ab243323 antibody), was detected at a molecular mass around 100 kDa in the validation western blot in lysates of MCT1 but not MCT2 cells. Thus, it is possible that in some, but not all, MCT cases on the TMA, a portion of the TET2 immunolabelling could be due to antibody recognition of this non-specific antigen. To address additional nonspecific staining problems that can arise an IHC,

both negative and positive controls were included. To best ensure staining that was identified in the TMA was due to antibody-antigen interaction, negative control TMA immunolabelling was performed (Kim et al., 2016). These TMA sections underwent the exact protocol as the TMA used for positive immunolabelling, except that no primary antibody was used. These negative controls were used to confirm that there was no non-specific binding of the secondary antibody to the tissue.

The benefit of using TMAs instead of single sections for each specimen is that a large patient cohort can be analyzed simultaneously with identical immunolabelling conditions, thus avoiding technical variability in the detection of target antigens in the tissues (Voduc et al., 2008). Constructing a TMA with 0.6 mm diameter cores from MCT donor blocks that are representative of the tumour section thus allows for detection of molecules that are clinically relevant to tumour phenotype (Sauter, 2010). However, in my study I encountered a problem that there was more core loss in the IDH1, IDH2, and TET2 stained TMAs than in the TMA sections used to detect 5MC, 5HMC, and DMNTs. The cores that were lost during processing were almost identical between the TMAs stained for TET2, IDH1, and IDH2. As these TMAs sections were the last ones to be cut, it could be that the cores did not reach as deep into the recipient block as the ones that remained. Since there were up to three cores taken from many cases, the loss of cores did not necessarily always lead to the loss of a case from further analysis. However if there was one core taken from a large tumour block and that does not capture the complete expression levels of the specimen, its loss can lead to missing relevant information (Sauter, 2010). Although there were many cases included in my study, for cases that had three cores taken from the tumour block, if only one remained after immunolabelling,

it could potentially affect the analysis. Arbitrary assessment of staining intensity by rating an IHC slide as weak, moderate, or strong staining can also lead to problems with variation between slides and impact the results (Voduc et al., 2008). Since a TMA was utilized and all cases were stained in one batch for any particular biomarker, the variation in how a case would be scored is thereby limited (Voduc et al., 2008). Although the scoring of the immunolabelling was not conducted by a trained pathologist the staining of all cases could still be directly compared to each other. Looking at all cores that were stained simultaneously in the TMA helped in stratifying the cases by directly comparing cores with high, medium, and low immunolabelling. Using QuPath (0.1.2) the brown DAB deposits and hematoxylin counterstaining were able to be deconvoluted into separate colour detections which aided in determining cellular staining intensity. Once the proper colour detection was set, background staining and chromogen staining could be analyzed separately allowing a clearer view of staining intensity. This allowed for a better stratification between high staining and low staining. Once parameters are set the program can then analyze each cell into the determined staining level and assign values to determine H-score for each core leading to more accurate results (Bankhead et al., 2017).

The next obvious step for this project would be to validate the prognostic power of my biomarkers in a prospective study. A prospective study would allow the ability to determine whether the markers are predictive of aggressive disease by following the patients as disease progresses. There can be bias in information available due to uncollected data that can occur in retrospective studies. For instance, missing data due to it not being recorded is less common for more clinically severe cases, as these are usually recorded more intensely than less clinically

severe cases (Talari & Goyal, 2020). As was seen in my study there were several cases with missing DFI and/or OS data. Data can be collected as the study progresses in prospective studies which is advantageous over retrospective studies (Talari & Goyal, 2020).

Additional areas to look at for future study could include determining whether increased D-2HG levels are associated with poorer DFI and shorter OS. In a normal state, the levels of D-2HG are very low as the very small amount that is produced is rapidly eliminated. In human cancer cases with mutant IDHs, D-2HG is detected in very high levels (Huang & Rao, 2014), so it would be valuable to study D-2HG levels in canine MCT. D-2HG levels are commonly detected by liquid chromatography or gas chromatography mass spectrometry (LC-MS, GC-MS)(Balss et al., 2012). As well, there exists a quicker enzymatic assay with similar detection sensitivity. This assay uses (D)-2-hydroxyglutarate dehydrogenase (HGDH) to convert D-2HG to αKG thereby accumulating NADH whose hydrogen is transferred to produce fluorescent resorufin by diaphorase (Balss et al., 2012). The detection of D-2HG levels in cells, frozen tissue, FFPE tissue, and body fluids yielded similar readouts to GC-MS (Balss et al., 2012). In many cancers mutation in IDHs is a gain of function mutation that leads to the increase in D-2HG levels (Figueroa et al., 2010). If the IDHs in MCTs have such gain of function mutations, then the levels of D-2HG may be higher in more aggressive MCTs.

Another step would be to evaluate whether hypomethylating agents such as Decitabine (5-aza-2'-deoxycytidine) can lead to changes in the methylation status of canine MCT cells in vitro, and to quantify the enzyme levels and activities in these treated cells. Hypomethylation agents are used in the treatment of various hematological malignancies such as AML and there is a precedent for utilizing TET2 and DNMT enzyme levels and mutations to determine

sensitivity to treatment (Bejar et al., 2014; Traina et al., 2014). Therefore, if hypomethylating agents are to be useful in the treatment of canine MCTs, levels of 5MC TET2, DNMTs, and IDHs in tumours could be potentially useful in identifying cases that would best respond to treatment.

**Summary and Conclusion**

In this study there was a statistically significant difference between the DFI and OS of canine MCTs immunolabelled for 5MC, DNMT1, DNMT3a, TET2, IDH1, and IDH2 when looking at all cases as well as when stratifying the cases by location or by intermediate grade. Low staining expression of TET2, IDH1, and IDH2 showed shorter DFI and OS in MCT cases when looking at intermediately graded tumours and specifically when stratifying by location in subcutaneous MCTs. Based on these results there may be significance in reduced and potentially altered enzyme expression of TET2 and IDHs in canine MCTs especially in subcutaneous MCTs. However, high staining levels for 5MC, DNMT1, and DNMT3a were associated with poorer DFI and OS when looking at all the cases of MCTs in this study as well as when stratifying the cases by location and intermediate grade. High levels of DNMT1 and DNMT3a staining were seen to be associated with shorter DFI and OS when looking at dermal MCTs. High 5MC staining levels were seen to be statistically associated with poorer DFI and OS when looking at all cases, in both dermal and subcutaneous cases and when looking at intermediately graded MCTs. Therefore, there may be significance in increased enzyme expression and activity of DNMT1 and DNMT3a in canine MCTs, especially in dermal MCTs. In addition, higher levels of 5MC or hypermethylation may be a robust indicator of poor prognosis in canine MCT.

## *REFERENCES*


Balss, J., Pusch, S., Beck, A.-C., Herold-Mende, C., Krämer, A., Thiede, C., Buckel, W., Langhans, C.-D., Okun, J. G., & Von Deimling, A. (2012). Enzymatic assay for quantitative analysis of (d)-2-hydroxyglutarate. *Acta Neuropathologica*, *124*(6), 883-891.

Bankhead, P., Loughrey, M. B., Fernández, J. A., Dombrowski, Y., Mcart, D. G., Dunne, P. D., Mcquaid, S., Gray, R. T., Murray, L. J., Coleman, H. G., James, J. A., Salto-Tellez, M., & Hamilton, P. W. (2017). QuPath: Open source software for digital pathology image analysis. *Scientific Reports*, *7*(1).

Bejar, R., Lord, A., Stevenson, K., Bar-Natan, M., Pérez-Ladaga, A., Zaneveld, J., Wang, H., Caughey, B., Stojanov, P., Getz, G., Garcia-Manero, G., Kantarjian, H., Chen, R., Stone, R. M., Neuberg, D., Steensma, D. P., & Ebert, B. L. (2014). TET2 mutations predict response to hypomethylating agents in myelodysplastic syndrome patients. *Blood*, *124*(17), 2705-2712.

Booth, D. G., Takagi, M., Sanchez-Pulido, L., Petfalski, E., Vargiu, G., Samejima, K., Imamoto, N., Ponting, C. P., Tollervey, D., Earnshaw, W. C., & Vagnarelli, P. (2014). Ki-67 is a PP1-interacting protein that organises the mitotic chromosome periphery. *eLife*, *3*.

Bostock, D., Crocker, J., Harris, K., & Smith, P. (1989). Nucleolar organiser regions as indicators of post-surgical prognosis in canine spontaneous mast cell tumours. *British Journal of Cancer*, *59*(6), 915-918.

Bronzini, I., Aresu, L., Paganin, M., Marchioretto, L., Comazzi, S., Cian, F., Riondato, F., Marconato, L., Martini, V., & Te Kronnie, G. (2017). DNA methylation and targeted sequencing of methyltransferases family genes in canine acute myeloid leukaemia, modelling human myeloid leukaemia. *Veterinary and Comparative Oncology*, *15*(3), 910-918.

Camp, R. L., Dolled-Filhart, M., & Rimm, D. L. (2004). X-tile: a new bio-informatics tool for biomarker assessment and outcome-based cut-point optimization. *Clin Cancer Res*, *10*(21), 7252-7259.

Challen, G. A., Sun, D., Jeong, M., Luo, M., Jelinek, J., Berg, J. S., Bock, C., Vasanthakumar, A., Gu, H., Xi, Y., Liang, S., Lu, Y., Darlington, G. J., Meissner, A., Issa, J.-P. J., Godley, L. A., Li, W., & Goodell, M. A. (2012). Dnmt3a is essential for hematopoietic stem cell differentiation. *Nature Genetics*, *44*(1), 23-31.

Chen, T., Ueda, Y., Dodge, J. E., Wang, Z., & Li, E. (2003). Establishment and Maintenance of Genomic Methylation Patterns in Mouse Embryonic Stem Cells by Dnmt3a and Dnmt3b. *Molecular and Cellular Biology*, *23*(16), 5594-5605.

Costa Casagrande, T. A., De Oliveira Barros, L. M., Fukumasu, H., Cogliati, B., Chaible, L. M., Dagli, M. L. Z., & Matera, J. M. (2015). The value of molecular expression of KIT and KIT ligand analysed using real-time polymerase chain reaction and immunohistochemistry as a prognostic indicator for canine cutaneous mast cell tumours. *Veterinary and Comparative Oncology*, *13*(1), 1-10.

Cui, J., Zheng, L., Zhang, Y., & Xue, M. (2021). Bioinformatics analysis of DNMT1 expression and its role in head and neck squamous cell carcinoma prognosis. *Scientific Reports*, *11*(1).

Da Silva, E. Z. M., Jamur, M. C., & Oliver, C. (2014). Mast Cell Function. *Journal of Histochemistry & Cytochemistry*, *62*(10), 698-738.

De Vita, S., Schneider, R. K., Garcia, M., Wood, J., Gavillet, M., Ebert, B. L., Gerbaulet, A., Roers, A., Levine, R. L., Mullally, A., & Williams, D. A. (2014). Loss of function of TET2 cooperates with constitutively active KIT in murine and human models of mastocytosis. *PLoS One*, *9*(5), e96209.

Derissen, E. J. B., Beijnen, J. H., & Schellens, J. H. M. (2013). Concise Drug Review: Azacitidine and Decitabine. *The Oncologist*, *18*(5), 619-624.

Dexheimer, G. M., Alves, J., Reckziegel, L., Lazzaretti, G., & Abujamra, A. L. (2017). DNA Methylation Events as Markers for Diagnosis and Management of Acute Myeloid Leukemia and Myelodysplastic Syndrome. *Disease Markers*, *2017*, 1-14.

Dey, P. (2018). Immunocytochemistry in Histology and Cytology. In *Basic and Advanced Laboratory Techniques in Histopathology and Cytology* (pp. 149-169). Springer Singapore.

Fedchenko, N., & Reifenrath, J. (2014). Different approaches for interpretation and reporting of immunohistochemistry analysis results in the bone tissue – a review. *Diagnostic Pathology*, *9*(1).

Figueroa, M. E., Abdel-Wahab, O., Lu, C., Ward, P. S., Patel, J., Shih, A., Li, Y., Bhagwat, N., Vasanthakumar, A., Fernandez, H. F., Tallman, M. S., Sun, Z., Wolniak, K., Peeters, J. K., Liu, W., Choe, S. E., Fantin, V. R., Paietta, E., Löwenberg, B., . . . Melnick, A. (2010). Leukemic IDH1 and IDH2 Mutations Result in a Hypermethylation Phenotype, Disrupt TET2 Function, and Impair Hematopoietic Differentiation. *Cancer Cell*, *18*(6), 553-567.

Flesner, B. K., Kumar, S. R., & Bryan, J. N. (2014). 6-Thioguanine and zebularine down-regulate DNMT1 and globally demethylate canine malignant lymphoid cells. *BMC Veterinary Research*, *10*(1).

Fuhrich, D. G., Lessey, B. A., & Savaris, R. F. (2013). Comparison of HSCORE assessment of endometrial beta3 integrin subunit expression with digital HSCORE using computerized image analysis (ImageJ). *Anal Quant Cytopathol Histpathol*, *35*(4), 210-216.

Fulcher, R. P., Ludwig, L. L., Bergman, P. J., Newman, S. J., Simpson, A. M., & Patnaik, A. K. (2006). Evaluation of a two-centimeter lateral surgical margin for excision of grade I and grade II cutaneous mast cell tumors in dogs. *Journal of the American Veterinary Medical Association*, *228*(2), 210-215.

Garrett, L. (2014). Canine mast cell tumors: diagnosis, treatment, and prognosis. *Veterinary Medicine: Research and Reports*, 49.

Giantin, M., Vascellari, M., Morello, E. M., Capello, K., Vercelli, A., Granato, A., Lopparelli, R. M., Nassuato, C., Carminato, A., Martano, M., Mutinelli, F., & Dacasto, M. (2012). c-KIT messenger RNA and protein expression and mutations in canine cutaneous mast cell tumors. *Journal of Veterinary Diagnostic Investigation*, *24*(1), 116-126.

Gil Da Costa, R. M. (2015). C-kit as a prognostic and therapeutic marker in canine cutaneous mast cell tumours: From laboratory to clinic. *The Veterinary Journal*, *205*(1), 5-10.

Greenberg, M. V. C., & Bourc'His, D. (2019). The diverse roles of DNA methylation in mammalian development and disease. *Nature Reviews Molecular Cell Biology*, *20*(10), 590-607.

Halsey, C. H. C., Thamm, D. H., Weishaar, K. M., Burton, J. H., Charles, J. B., Gustafson, D. L., Avery, A. C., & Ehrhart, E. J. (2017). Expression of Phosphorylated KIT in Canine Mast Cell Tumor. *Vet Pathol*, *54*(3), 387-394.

Hassan, S., Ferrario, C., Mamo, A., & Basik, M. (2007). Tissue microarrays: emerging standard for biomarker validation. *Current opinion in biotechnology*, *19*(1), 19-25.

Horta, R. S., Lavalle, G. E., Monteiro, L. N., Souza, M. C. C., Cassali, G. D., & Araújo, R. B. (2018). Assessment of Canine Mast Cell Tumor Mortality Risk Based on Clinical, Histologic, Immunohistochemical, and Molecular Features. *Veterinary Pathology*, *55*(2), 212-223.

Huang, Y., & Rao, A. (2014). Connections between TET proteins and aberrant DNA modification in cancer. *Trends in Genetics*, *30*(10), 464-474.

Itoh, T., Kojimoto, A., Uchida, K., Chambers, J., & Shii, H. (2021). Long-term postsurgical outcomes of mast cell tumors resected with a margin proportional to the tumor diameter in 23 dogs. *Journal of Veterinary Medical Science*, *83*(2), 230-233.

Janardhan, K. S., Jensen, H., Clayton, N. P., & Herbert, R. A. (2018). Immunohistochemistry in Investigative and Toxicologic Pathology. *Toxicologic Pathology*, *46*(5), 488-510.

Jawhar, N. M. T. (2009). Tissue Microarray: A rapidly evolving diagnostic and research tool. *Annals of Saudi medicine*, *29*(2), 123-127.

Kim, S.-W., Roh, J., & Park, C.-S. (2016). Immunohistochemistry for Pathologists: Protocols, Pitfalls, and Tips. *Journal of Pathology and Translational Medicine*, *50*(6), 411-418.

Kiupel, M., & Camus, M. (2019). Diagnosis and Prognosis of Canine Cutaneous Mast Cell Tumors. *Veterinary Clinics of North America: Small Animal Practice*, *49*(5), 819-836.

Kiupel, M., Webster, J. D., Bailey, K. L., Best, S., DeLay, J., Detrisac, C. J., Fitzgerald, S. D., Gamble, D., Ginn, P. E., Goldschmidt, M. H., Hendrick, M. J., Howerth, E. W., Janovitz, E. B., Langohr, I., Lenz, S. D., Lipscomb, T. P., Miller, M. A., Misdorp, W., Moroff, S., . . . Miller, R. (2011). Proposal of a 2-tier histologic grading system for canine cutaneous mast cell tumors to more accurately predict biological behavior. *Vet Pathol*, *48*(1), 147-155.

Kiupel, M., Webster, J. D., Kaneene, J. B., Miller, R., & Yuzbasiyan-Gurkan, V. (2004). The Use of KIT and Tryptase Expression Patterns as Prognostic Tools for Canine Cutaneous Mast Cell Tumors. *Veterinary Pathology*, *41*(4), 371-377.

Knight, B. J., Wood, G. A., Foster, R. A., & Coomber, B. L. (2021). Beclin-1 is a novel predictive biomarker for canine cutaneous and subcutaneous mast cell tumors. *Veterinary Pathology*, Sep 14; 030098582110425.

Ko, M., An, J., Pastor, W. A., Koralov, S. B., Rajewsky, K., & Rao, A. (2015). TET proteins and 5-methylcytosine oxidation in hematological cancers. *Immunological Reviews*, *263*(1), 6-21.

Krick, E. L., Billings, A. P., Shofer, F. S., Watanabe, S., & Sorenmo, K. U. (2009). Cytological lymph node evaluation in dogs with mast cell tumours: association with grade and survival. *Veterinary & comparative oncology*, *7*(2), 130-138.

Kroeze, L. I., van der Reijden, B. A., & Jansen, J. H. (2015). 5-Hydroxymethylcytosine: An epigenetic mark frequently deregulated in cancer. *Biochim Biophys Acta*, *1855*(2), 144-154.

Leoni, C., Montagner, S., Rinaldi, A., Bertoni, F., Polletti, S., Balestrieri, C., & Monticelli, S. (2017). Dnmt3arestrains mast cell inflammatory responses. *Proceedings of the National Academy of Sciences*, *114*(8), E1490-E1499.

Letard, S., Yang, Y., Hanssens, K., Palmérini, F., Leventhal, P. S., Guéry, S., Moussy, A., Kinet, J.-P., Hermine, O., & Dubreuil, P. (2008). Gain-of-Function Mutations in the Extracellular Domain of KIT Are Common in Canine Mast Cell Tumors. *Molecular Cancer Research*, *6*(7), 1137-1145.

London, C. A., Malpas, P. B., Wood-Follis, S. L., Boucher, J. F., Rusk, A. W., Rosenberg, M. P., Henry, C. J., Mitchener, K. L., Klein, M. K., Hintermeister, J. G., Bergman, P. J., Couto, G. C., Mauldin, G. N., & Michels, G. M. (2009). Multi-center, Placebo-controlled, Double-blind, Randomized Study of Oral Toceranib Phosphate (SU11654), a Receptor Tyrosine Kinase Inhibitor, for the Treatment of Dogs with Recurrent (Either Local or Distant) Mast Cell Tumor Following Surgical Excision. *Clinical Cancer Research*, *15*(11), 3856-3865.

Ma, H.-S., Wang, E. L., Xu, W.-F., Yamada, S., Yoshimoto, K., Qian, Z. R., Shi, L., Liu, L.-L., & Li, X.-H. (2018). Overexpression of DNA (Cytosine-5)-Methyltransferase 1 (DNMT1) And DNA (Cytosine-5)-Methyltransferase 3A (DNMT3A) Is Associated with Aggressive Behavior and Hypermethylation of Tumor Suppressor Genes in Human Pituitary Adenomas. *Medical Science Monitor*, *24*, 4841-4850.

Magaki, S., Hojat, S. A., Wei, B., So, A., & Yong, W. H. (2019). An Introduction to the Performance of Immunohistochemistry. In *Methods in Molecular Biology* (pp. 289-298). Springer New York.

Meng, H., Cao, Y., Qin, J., Song, X., Zhang, Q., Shi, Y., & Cao, L. (2015). DNA Methylation, Its Mediators and Genome Integrity. *International Journal of Biological Sciences*, *11*(5), 604-617.

Mizuno, S.-I., Chijiwa, T., Okamura, T., Akashi, K., Fukumaki, Y., Niho, Y., & Sasaki, H. (2001). Expression of DNA methyltransferases DNMT1,3A, and 3B in normal hematopoiesis and in acute and chronic myelogenous leukemia. *Blood*, *97*(5), 1172-1179.

Montagner, S., Leoni, C., Emming, S., Della Chiara, G., Balestrieri, C., Barozzi, I., Piccolo, V., Togher, S., Ko, M., Rao, A., Natoli, G., & Monticelli, S. (2016). TET2 Regulates Mast Cell Differentiation and Proliferation through Catalytic and Non-catalytic Activities. *Cell Reports*, *15*(7), 1566-1579.

Morimoto, C. Y., Tedardi, M. V., da Fonseca, I. I. M., Kimura, K. C., Sanches, D. S., Epiphanio, T. F., de Francisco Strefezzi, R., & Dagli, M. L. Z. (2017). Evaluation of the global DNA methylation in canine mast cell tumour samples by immunostaining of 5-methyl cytosine. *Vet Comp Oncol*, *15*(3), 1014-1018.

Murphy, S., Sparkes, A. H., Blunden, A. S., Brearley, M. J., & Smith, K. C. (2006). Effects of stage and number of tumours on prognosis of dogs with cutaneous mast cell tumours. *Veterinary Record*, *158*(9), 287-291.

Olsen, J. A., Thomson, M., O'Connell, K., & Wyatt, K. (2018). Combination vinblastine, prednisolone and toceranib phosphate for treatment of grade II and III mast cell tumours in dogs. *Veterinary Medicine and Science*, *4*(3), 237-251.

Patnaik, A. K., Ehler, W. J., & Macewen, E. G. (1984). Canine Cutaneous Mast Cell Tumor: Morphologic Grading and Survival Time in 83 Dogs. *Veterinary Pathology*, *21*(5), 469-474.

Qu, X., Davison, J., Du, L., Storer, B., Stirewalt, D. L., Heimfeld, S., Estey, E., Appelbaum, F. R., & Fang, M. (2015). Identification of differentially methylated markers among cytogenetic risk groups of acute myeloid leukemia. *Epigenetics*, *10*(6), 526-535.

Ramos-Vara, J. A. (2017). Principles and Methods of Immunohistochemistry. In *Methods in Molecular Biology* (pp. 115-128). Springer New York.

Rasmussen, K. D., Jia, G., Johansen, J. V., Pedersen, M. T., Rapin, N., Bagger, F. O., Porse, B. T., Bernard, O. A., Christensen, J., & Helin, K. (2015). Loss ofTET2in hematopoietic cells leads to DNA hypermethylation of active enhancers and induction of leukemogenesis. *Genes & Development*, *29*(9), 910-922.

Reszka, E., Jabłońska, E., Wieczorek, E., Valent, P., Arock, M., Nilsson, G., Nedoszytko, B., & Niedoszytko, M. (2021). Epigenetic Changes in Neoplastic Mast Cells and Potential Impact in Mastocytosis. *International Journal of Molecular Sciences*, *22*(6), 2964.

Romansik, E. M., Reilly, C. M., Kass, P. H., Moore, P. F., & London, C. A. (2007). Mitotic Index Is Predictive for Survival for Canine Cutaneous Mast Cell Tumors. *Veterinary Pathology*, *44*(3), 335-341.

Sabattini, S., Scarpa, F., Berlato, D., & Bettini, G. (2015). Histologic grading of canine mast cell tumor: is 2 better than 3? *Vet Pathol*, *52*(1), 70-73.

Sauter, G. (2010). Representativity of TMA Studies. In *Methods in Molecular Biology* (pp. 27-35). Humana Press.

Scholzen, T., & Gerdes, J. (2000). The Ki-67 protein: From the known and the unknown. *Journal of cellular physiology*, *182*(3), 311-322.

Scopim-Ribeiro, R., Machado-Neto, J. A., Campos, P. D. M., Silva, C. A. M., Favaro, P., Lorand-Metze, I., Costa, F. F., Saad, S. T. O., & Traina, F. (2015). Ten-Eleven-Translocation 2 (TET2) is downregulated in myelodysplastic syndromes. *European Journal of Haematology*, *94*(5), 413-418.

Selmic, L. E., & Ruple, A. (2020). A systematic review of surgical margins utilized for removal of cutaneous mast cell tumors in dogs. *BMC Veterinary Research*, *16*(1).

Sledge, D. G., Webster, J., & Kiupel, M. (2016). Canine cutaneous mast cell tumors: A combined clinical and pathologic approach to diagnosis, prognosis, and treatment selection. *Vet J*, *215*, 43-54.

Sobecki, M., Mrouj, K., Camasses, A., Parisis, N., Nicolas, E., Llères, D., Gerbe, F., Prieto, S., Krasinska, L., David, A., Eguren, M., Birling, M.-C., Urbach, S., Hem, S., Déjardin, J., Malumbres, M., Jay, P., Dulic, V., Lafontaine, D. L., . . . Fisher, D. (2016). The cell proliferation antigen Ki-67 organises heterochromatin. *eLife*, *5*.

Stefanello, D., Buracco, P., Sabattini, S., Finotello, R., Giudice, C., Grieco, V., Iussich, S., Tursi, M., Scase, T., Di Palma, S., Bettini, G., Ferrari, R., Martano, M., Gattino, F., Marrington, M., Mazzola, M., Elisabetta Vasconi, M., Annoni, M., & Marconato, L. (2015). Comparison of 2- and 3-category histologic grading systems for predicting the presence of metastasis at the time of initial

evaluation in dogs with cutaneous mast cell tumors: 386 cases (2009-2014). *J Am Vet Med Assoc*, *246*(7), 765-769.

Tajima, S., Suetake, I., Takeshita, K., Nakagawa, A., & Kimura, H. (2016). Domain Structure of the Dnmt1, Dnmt3a, and Dnmt3b DNA Methyltransferases. In *Advances in Experimental Medicine and Biology* (pp. 63-86). Springer International Publishing.

Takeuchi, Y., Fujino, Y., Watanabe, M., Takahashi, M., Nakagawa, T., Takeuchi, A., Bonkobara, M., Kobayashi, T., Ohno, K., Uchida, K., Asano, K., Nishimura, R., Nakayama, H., Sugano, S., Ohashi, Y., & Tsujimoto, H. (2013). Validation of the prognostic value of histopathological grading or c-kit mutation in canine cutaneous mast cell tumours: A retrospective cohort study. *The Veterinary Journal*, *196*(3), 492-498.

Talari, K., & Goyal, M. (2020). Retrospective studies - utility and caveats. *The Journal of the Royal College of Physicians of Edinburgh*, *50*(4), 398-402.

Thamm, D. H., Avery, A. C., Berlato, D., Bulman-Fleming, J., Clifford, C. A., Hershey, A. E., Intile, J. L., Jones, P. D., Kamstock, D. A., Liptak, J. M., Pavuk, A., Peauroi, J., Powell, R., Rissetto, K., Valli, V. E. O., & Webster, J. D. (2019). Prognostic and predictive significance of KIT protein expression and c-kit gene mutation in canine cutaneous mast cell tumours: A consensus of the Oncology-Pathology Working Group. *Veterinary and Comparative Oncology*, *17*(4), 451-455.

Thamm, D. H., Turek, M. M., & Vail, D. M. (2006). Outcome and Prognostic Factors Following Adjuvant Prednisone/Vinblastine Chemotherapy for High-Risk Canine Mast Cell Tumour: 61 Cases. *Journal of Veterinary Medical Science*, *68*(6), 581-587.

Thompson, J. J., Pearl, D. L., Yager, J. A., Best, S. J., Coomber, B. L., & Foster, R. A. (2011). Canine Subcutaneous Mast Cell Tumor. *Veterinary Pathology*, *48*(1), 156-168.

Thompson, J. J., Yager, J. A., Best, S. J., Pearl, D. L., Coomber, B. L., Torres, R. N., Kiupel, M., & Foster, R. A. (2011). Canine Subcutaneous Mast Cell Tumors. *Veterinary Pathology*, *48*(1), 169-181.

Traina, F., Visconte, V., Elson, P., Tabarroki, A., Jankowska, A. M., Hasrouni, E., Sugimoto, Y., Szpurka, H., Makishima, H., O'Keefe, C. L., Sekeres, M. A., Advani, A. S., Kalaycio, M., Copelan, E. A., Saunthararajah, Y., Olalla Saad, S. T., Maciejewski, J. P., & Tiu, R. V. (2014). Impact of molecular mutations on treatment response to DNMT inhibitors in myelodysplasia and related neoplasms. *Leukemia*, *28*(1), 78-87.

Traina, F., Visconte, V., Jankowska, A. M., Makishima, H., O'Keefe, C. L., Elson, P., Han, Y., Hsieh, F. H., Sekeres, M. A., Mali, R. S., Kalaycio, M., Lichtin, A. E., Advani, A. S., Duong, H. K., Copelan, E., Kapur, R., Olalla Saad, S. T., Maciejewski, J. P., & Tiu, R. V. (2012). Single Nucleotide Polymorphism Array Lesions, TET2, DNMT3A, ASXL1 and CBL Mutations Are Present in Systemic Mastocytosis. *PLoS One*, *7*(8), e43090.

Trowbridge, J. J., Snow, J. W., Kim, J., & Orkin, S. H. (2009). DNA Methyltransferase 1 Is Essential for and Uniquely Regulates Hematopoietic Stem and Progenitor Cells. *Cell Stem Cell*, *5*(4), 442-449.

Turcan, S., Fabius, A. W. M., Borodovsky, A., Pedraza, A., Brennan, C., Huse, J., Viale, A., Riggins, G. J., & Chan, T. A. (2013). Efficient induction of differentiation and growth inhibition in IDH1 mutant glioma cells by the DNMT Inhibitor Decitabine. *Oncotarget*, *4*(10), 1729-1736.

Valent, P., Akin, C., Hartmann, K., Nilsson, G., Reiter, A., Hermine, O., Sotlar, K., Sperr, W. R., Escribano, L., George, T. I., Kluin-Nelemans, H. C., Ustun, C., Triggiani, M., Brockow, K., Gotlib, J., Orfao, A., Kovanen, P. T., Hadzijusufovic, E., Sadovnik, I., . . . Galli, S. J. (2020). Mast cells as a unique hematopoietic lineage and cell system: From Paul Ehrlich's visions to precision medicine concepts. *Theranostics*, *10*(23), 10743-10768.

Van Diest, P. J., Brugal, G., & Baak, J. P. (1998). Proliferation markers in tumours: interpretation and clinical value. *Journal of Clinical Pathology*, *51*(10), 716-724.

Voduc, D., Kenney, C., & Nielsen, T. O. (2008). Tissue Microarrays in Clinical Oncology. *Seminars in Radiation Oncology*, *18*(2), 89-97.

Waitkus, M. S., Diplas, B. H., & Yan, H. (2018). Biological Role and Therapeutic Potential of IDH Mutations in Cancer. *Cancer Cell*, *34*(2), 186-195.

Warland, J., Brioschi, V., Owen, L., & Dobson, J. (2015). Canine mast cell tumours: decision-making and treatment. *In Practice*, *37*(7), 315-332.

Webster, J. D., Yuzbasiyan-Gurkan, V., Miller, R. A., Kaneene, J. B., & Kiupel, M. (2007). Cellular Proliferation in Canine Cutaneous Mast Cell Tumors: Associations withc-KITand Its Role in Prognostication. *Veterinary Pathology*, *44*(3), 298-308.

Welle, M. M., Bley, C. R., Howard, J., & Rüfenacht, S. (2008). Canine mast cell tumours: a review of the pathogenesis, clinical features, pathology and treatment. *Vet Dermatol*, *19*(6), 321-339.

Wong, K. K., Lawrie, C. H., & Green, T. M. (2019). Oncogenic Roles and Inhibitors of DNMT1, DNMT3A, and DNMT3B in Acute Myeloid Leukaemia. *Biomarker Insights*, *14*, 117727191984645.

Xu, W., Yang, H., Liu, Y., Yang, Y., Wang, P., Kim, S.-H., Ito, S., Yang, C., Wang, P., Xiao, M.-T., Liu, L.-X., Jiang, W.-Q., Liu, J., Zhang, J.-Y., Wang, B., Frye, S., Zhang, Y., Xu, Y.-H., Lei, Q.-Y., . . . Xiong, Y. (2011). Oncometabolite 2-Hydroxyglutarate Is a Competitive Inhibitor of α-Ketoglutarate-Dependent Dioxygenases. *Cancer Cell*, *19*(1), 17-30.

Yin, X., & Xu, Y. (2016). Structure and Function of TET Enzymes. In *Advances in Experimental Medicine and Biology* (pp. 275-302). Springer International Publishing.

Zemke, D., Yamini, B., & Yuzbasiyan-Gurkan, V. (2002). Mutations in the Juxtamembrane Domain of c-KIT Are Associated with Higher Grade Mast Cell Tumors in Dogs. *Veterinary Pathology*, *39*(5), 529-535.

Zhang, T. J., Zhou, J. D., Yang, D. Q., Wang, Y. X., Wen, X. M., Guo, H., Yang, L., Lian, X. Y., Lin, J., & Qian, J. (2018). TET2 expression is a potential prognostic and predictive biomarker in cytogenetically normal acute myeloid leukemia. *Journal of Cellular Physiology*, *233*(8), 5838-5846.

## *Appendix*

### *Appendix 1 - Preparation of Materials*

Electrophoresis running buffer:

1X running buffer was made from a 10X stock diluted in MilliQ. 10x stock: 144.2 g Glycine, 30.2 g Tris-base, 50.0 mL of 20% SDS dissolved in MilliQ water to a final volume of 1000 mL, with pH adjusted to 8.3 using HCL.

Transfer buffer:

200 mL of Methanol, 80 mL of Towbin Solution, 0.2mL of 20% SDS added to 720mL of MilliQ water for a final volume of 1000mL. (*Towbin solution*: 144.1 g Glycine + 30.25 g of Tris-base dissolved in MilliQ water to a final volume of 1000 mL).

Modified transfer buffer for larger molecular weight target protein:

100 mL of Methanol, 80 mL of *Towbin* Solution, 0.5 mL of 20% SDS added to 820 mL of MilliQ water for a final volume of 1000 mL.

Tris-Buffered Saline-Tween 20 (TBS-T):

1X TBS-T was diluted in MilliQ from a 20x stock. 20X TBS-T: 175.32 g NaCl, 48.46 g Tris-base, 10 mL of Tween-20 dissolved in MilliQ water to a final volume of 1000 mL, with pH adjusted to 7.6 using HCL.

Blocking solution:

5% Blocking Agent (Skim milk powder/IgG-free BSA) in 1X TBS-T.

10 mM Citrate Buffer, pH 6.0 (1000 mL):

Made by combining 18.0 mL Stock Solution A and 82.0 mL Stock Solution B and $dH_2O$ to a final volume of 1000 mL, with pH adjusted to 6.0 using HCL.

*Stock solution A:* 1.92g citric Acid in 100 mL $dH_2O$.

*Stock solution B:* 14.7g sodium citrate dihydrate in 500 mL $dH_2O$.

EDTA pH 9.0:

Dako Target Retrieval Solution, pH 9, Tris/EDTA buffer 10X was diluted to 1Xin $dH_2O$.

Tris Buffer

50 mM tris base, 150 mM NaCl and 0.01% Triton X-100 in MilliQ water

6.06 g tris base, 8.77 g NaCl, 100 µL Triton X-100 in a final volume of 1000 mL with a pH adjusted to 7.6.

Acid alcohol solution:

175 mL Isopropanol, 2.5 mL HCL, 72.5 mL $dH_2O$.

Ammonium water

5 drops ammonium hydroxide in 250 mL $dH_2O$.

***Appendix 2 - IHC conditions***

| Immunolabelling target | Antigen retrieval | 3.5M HCL incubation (minutes) | 3% hydrogen peroxide blocking (minutes) | 1% normal goat blocking (minutes) | Primary antibody dilution | Primary antibody incubation | DAB incubation (minutes) |
|---|---|---|---|---|---|---|---|
| 5MC | 10 mM sodium citrate buffer, pH 6.0 for 20 minutes at 95°C | 15 | 3 | 10 | 1 µg/mL | 4°C overnight in humidity chamber | 15 |
| 5HMC | EDTA pH 9.0 for 20 minutes at 95°C | 15 | 3 | 10 | 1:2000 | 4°C overnight in humidity chamber | 15 |
| DNMT1 | 10 mM sodium citrate buffer, pH 6.0 for 20 minutes at 95°C | NA | 3 | 10 | 1:100 | 4°C overnight in humidity chamber | 15 |
| DNMT3a | 10 mM sodium citrate buffer, pH 6.0 for 20 minutes at 95°C | NA | 3 | 10 | 1:200 | 4°C overnight in humidity chamber | 15 |
| TET2 | 10 mM sodium citrate buffer, pH 6.0 for 20 minutes at 95°C | NA | 3 | 10 | 1:50 | 2 hours at 37°C | 15 |
| IDH1 | 10 mM sodium citrate buffer, pH 6.0 for 20 minutes at 95°C | NA | 3 | 10 | 1:100 | 4°C overnight in humidity chamber | 6 |
| IDH2 | 10 mM sodium citrate buffer, pH 6.0 for 20 minutes at 95°C | NA | 3 | 10 | 1:100 | 4°C overnight in humidity chamber | 6 |

## *Appendix 3 - QuPath parameters*

5MC QuPath parameters

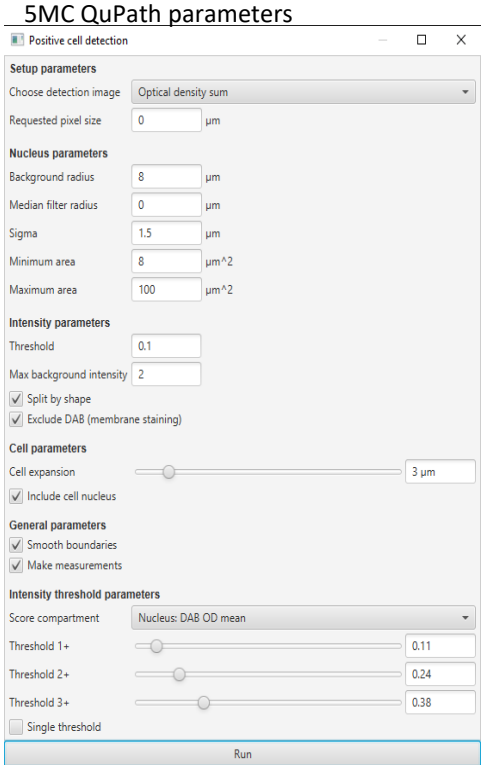


5HMC QuPath parameters

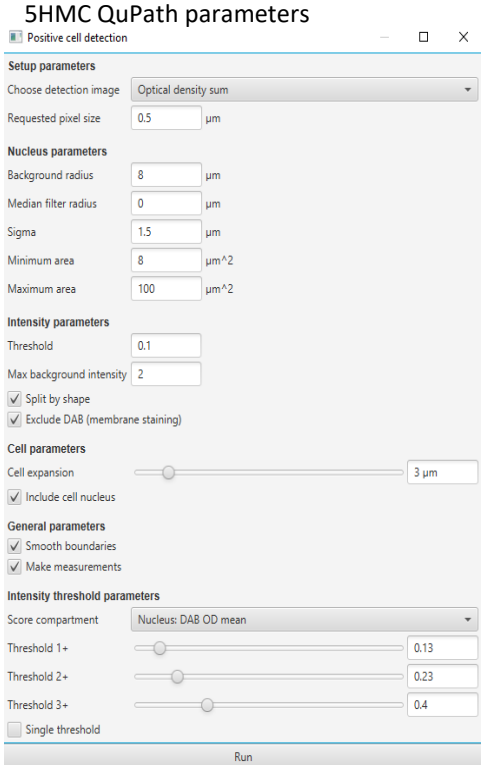


DNMT1 QuPath parameters

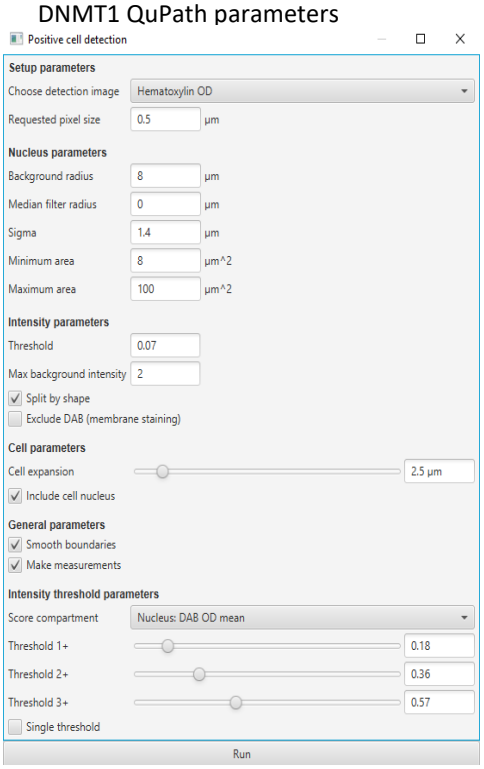


DNMT3a QuPath parameters

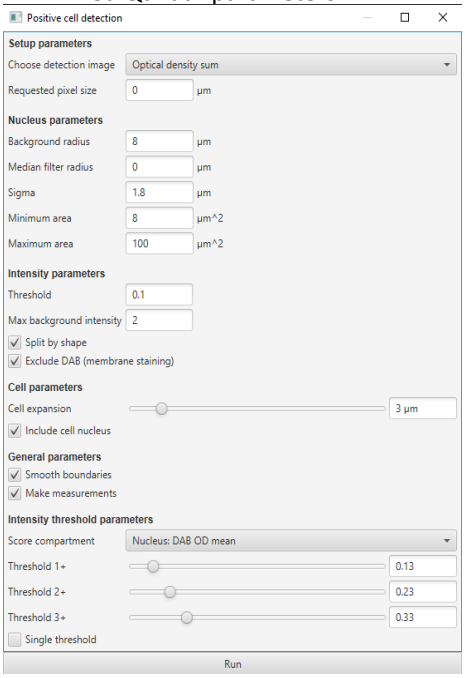


TET2 QuPath parameters

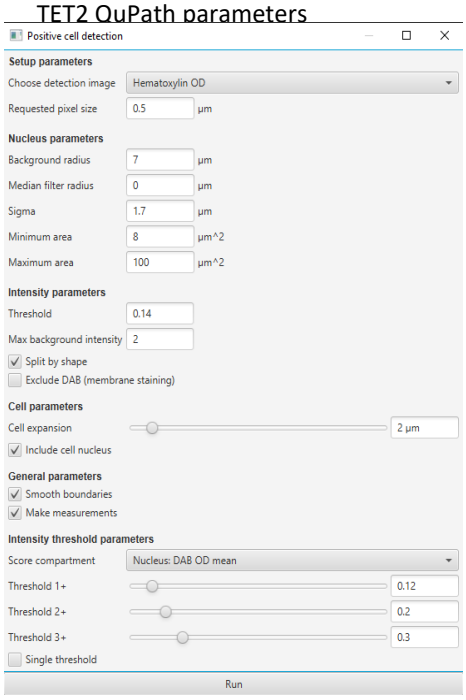


IDH1 QuPath parameters

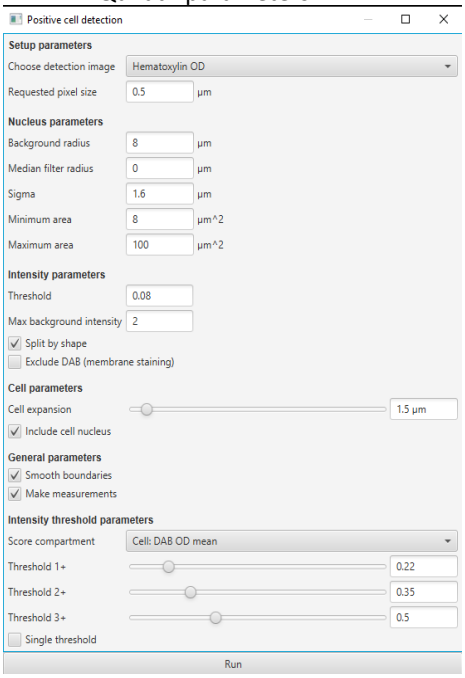

IDH2 QuPath parameters

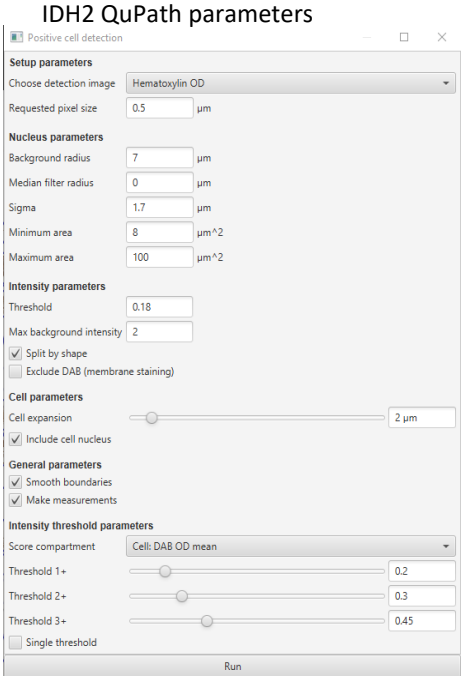


**Appendix 3:** Parameters inputted into QuPath for detection and staining for each of the markers.

***Appendix 4 – Correlation analysis and t-tests***

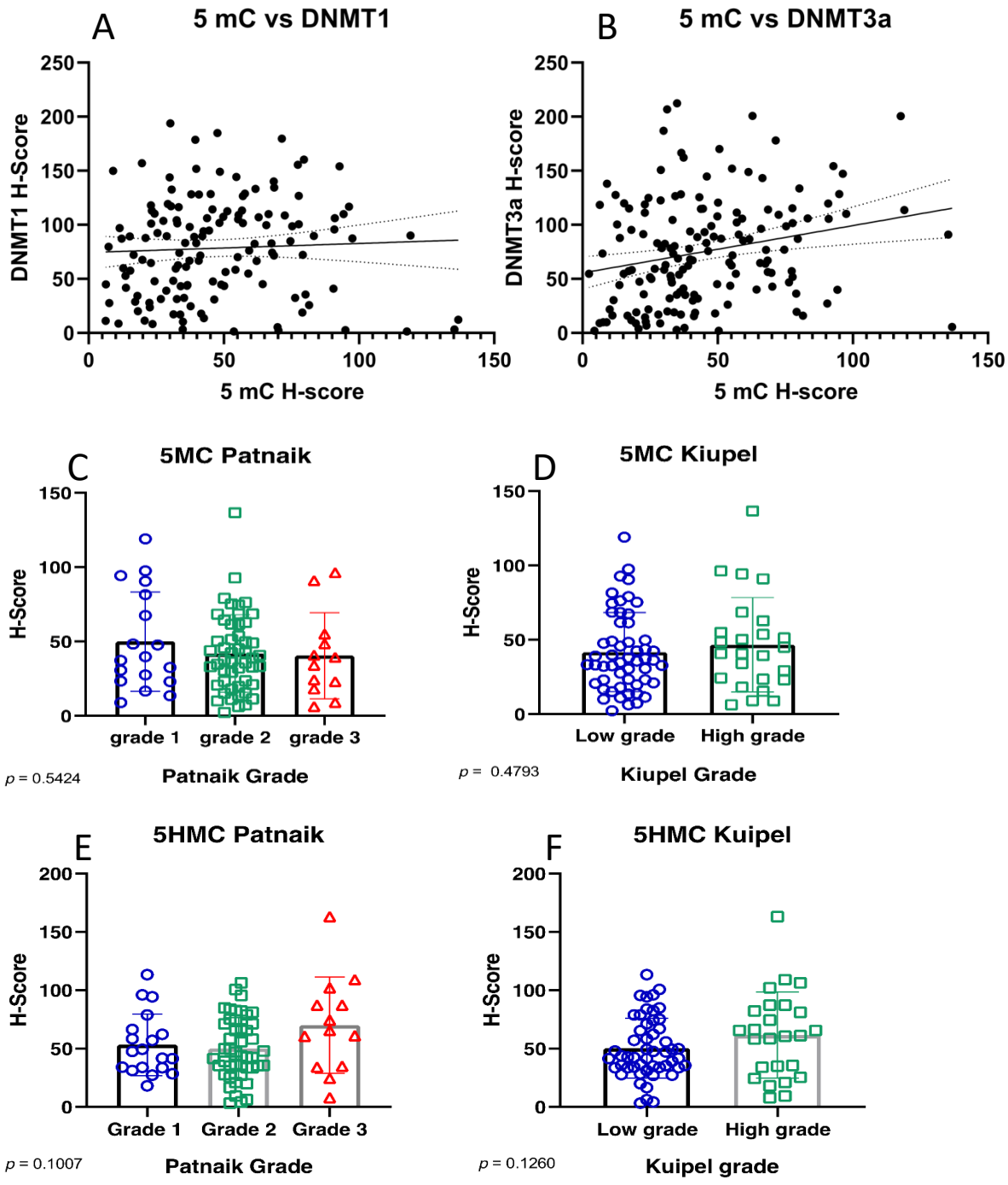


**Appendix 4:** (A) correlation analysis of H-score staining intensities between DNMT1 and 5MC immunolabelled cases. (B) correlation analysis of H-score staining intensities between DNMT3a and 5MC immunolabelled cases. T-tests comparing the level of stainig intensities of the cases grouped by Patnaik or Kiupel grading, (C) 5MC H-Scores grouped by Patnaik grade, (D) 5MC H-scores grouped by Kiupel grade, (E) 5HMC H-Scores grouped by Patnaik grade, (F) 5HMC H-scores grouped by Kiupel grade.